331
11/18/80

Lb. 528

ornl

ORNL/TM-6445

OAK
RIDGE
NATIONAL
LABORATORY

UNION
CARBIDE

Separation of Americium, Curium, and Rare Earths from High-Level Wastes by Oxalate Precipitation: Experiments with Synthetic Waste Solutions

C. W. Forsberg

MASTER

OPERATED BY
UNION CARBIDE CORPORATION
FOR THE UNITED STATES
DEPARTMENT OF ENERGY

DISCLAIMER

Printed in the United States of America. Available from
National Technical Information Service
U.S. Department of Commerce
5285 Port Royal Road, Springfield, Virginia 22161
NTIS price codes—Printed Copy: A06 Microfiche A01

ORNL/TM-6445
Dist. Category UC-70

Contract No. W-7405-eng-26

CHEMICAL TECHNOLOGY DIVISION

SEPARATION OF AMERICIUM, CURIUM, AND RARE EARTHS FROM HIGH-LEVEL WASTES BY OXALATE PRECIPITATION: EXPERIMENTS WITH SYNTHETIC WASTE SOLUTIONS

C. W. Forsberg

Date Published: January 1980

OAK RIDGE NATIONAL LABORATORY
Oak Ridge, Tennessee 37830
operated by
UNION CARBIDE CORPORATION
for the
DEPARTMENT OF ENERGY

THIS PAGE

WAS INTENTIONALLY

LEFT BLANK

CONTENTS

SEPARATION OF AMERICIUM, CURIUM, AND RARE EARTHS FROM HIGH-LEVEL WASTES BY OXALATE PRECIPITATION: EXPERIMENTS WITH SYNTHETIC WASTE SOLUTIONS

C. W. Forsberg

ABSTRACT

The separation of trivalent actinides and rare earths from other fission products in high-level nuclear wastes by oxalate precipitation followed by ion exchange (OPIX) was experimentally investigated using synthetic wastes and a small-scale, continuous-flow oxalic acid precipitation and solid-liquid separation system. Trivalent actinide and rare earth oxalates are relatively insoluble in 0.5 to 1.0 M HNO_3 whereas other fission product oxalates are not. The continuous-flow system consisted of one or two stirred-tank reactors in series for crystal growth. Oxalic acid and waste solutions were mixed in the first tank, with the product solid-liquid slurry leaving the second tank. Solid-liquid separation was tested by filters and by a gravity settler. The experiments determined the fraction of rare earths precipitated and separated from synthetic waste streams as a function of number of reactors, system temperature, oxalic acid concentration, liquid residence time in the process, power input to the stirred-tank reactors, and method of solid-liquid separation. The crystalline precipitate was characterized with respect to form, size, and chemical composition. These experiments are only the first step in converting a proposed chemical flowsheet into a process flowsheet suitable for large-scale remote operations at high activity levels.

---

1. SUMMARY

The separation of trivalent actinides and lanthanides from synthetic high-level wastes (HLW) by precipitation with oxalic acid was investigated using continuous-flow equipment. This process is one step in a multistep process to remove all actinides from HLW and hence reduce the potential long-term risks associated with geological isolation of these wastes. The experiments were an initial effort to develop methods that will permit the remote use of the OPIX process in a large-scale facility at high activity levels.

In the OPIX (oxalate precipitation followed by ion exchange) process, the HLW solution from a Purex-type reprocessing plant and a pure oxalic acid solution flow independently into the first of one or more stirred-tank reactors (STRs) in series. The rare earths and trivalent actinides combine with the oxalate ion to produce insoluble oxalate crystals. The precipitated rare earths and actinides (about 1% of the volume of liquid) are removed by a solid-liquid separation device. Residual trivalent actinides (about 10% of the total) are removed from the mother liquor by ion exchange; however, this part of the process was not tested in the experimental work reported here.

The following experimental variables were investigated: number of STRs (one or two), liquid residence time per reactor (15 to 40 min), system temperature (25 to 50°C), final concentration of oxalic acid waste (0.2 to 0.3 M), energy input to stirrer (0.02 to 0.18 W/liter), and method of solid-liquid separation. Product yields varied from 46 to 92%. The best set of operating conditions within the range of variables investigated was two STRs in series; liquid residence time per reactor, ≥40 min; operating temperature, ≤25°C; and oxalic acid feed concentration, ≥0.45 M, yielding a final solution concentration ≥0.3 M. The stirrer speed of STR No. 1 did not affect the product yield significantly, but higher stirrer speeds (0.18 W/liter) were desirable for STR No. 2. Although solid-liquid separation by settling was not satisfactory, efficient separations were obtained by filtration. Product yields (defined as the percent of the rare earths in the feed collected as a solid) varied from 90 to 92% after passing through 12-, 5-, and 1-μm filters in series. Particle-size distributions and other observations suggest that the optimum solid-liquid separation device for a full-scale plant may be a continuous centrifuge, although filters yield excellent results. It was not determined whether filtrates contained particles that were less than 1 μm in diameter.

Chemical analysis revealed that, in addition to the rare earths, the precipitate contained the following percentages of the feed solution elements: barium, 0.6%; strontium, 1.3%; ruthenium, 1%; molybdenum, 0.2%; and zirconium, 5.2%.

From this initial experimental data it appears that a continuous process can be developed for use in large-scale, radioactive operations in which oxalate precipitation is used to remove the bulk of the trivalent actinides and rare earths from HLW as part of the OPIX process.

2. INTRODUCTION

The purpose of this study was to determine the feasibility of continuously carrying out the oxalate precipitation step in the OPIX process using nonradioactive synthetic waste solutions. This study represents the first step of an evaluation of the adaptability of continuous oxalate precipitation to fully remote processing. Specific objectives of the experimental investigation were (1) to select the most promising type of continuous precipitation equipment, based on process requirements, and test it in potentially feasible process configurations (i.e., single or multiple units), and (2) to determine the yield and purity of the oxalate precipitate in terms of both equipment and chemical parameters.

Although the intense radiation associated with HLW (Fig. 1) is also expected to have significant effects, it is first necessary to demonstrate that the continuous precipitation concept is basically sound. Important effects expected from the intense radiation are generation of heat within the precipitate and conversion of oxalate ions to gaseous CO_2 and H_2O.

This work was carried out as part of a program on the evaluation of the technical feasibility of partitioning and transmutation as a waste management concept.[1] In this waste management concept, actinides (and perhaps other long-lived radionuclides such as ^{129}I) are removed from waste streams and then are transmuted (by neutron capture or fissioning) to shorter-lived radionuclides. The purpose of partitioning and transmutation is to reduce the potential risks associated with the long-term (>500-year) geologic isolation of nuclear wastes and has been discussed in detail by several investigators.[1-4] Oxalate precipitation is only one step in the overall flowsheet for removing actinides from wastes, and only those portions of the flowsheet which are necessary to the understanding of the OPIX chemistry and operations will be reported here.

In the conceptual flowsheet for actinide partitioning and transmutation (Fig. 2), the Purex process is modified to give improved recoveries of uranium and plutonium from spent fuel and to also recover neptunium. In conventional reprocessing using Purex, about 99.5% of the uranium and plutonium are recovered, whereas the neptunium, americium, curium, and

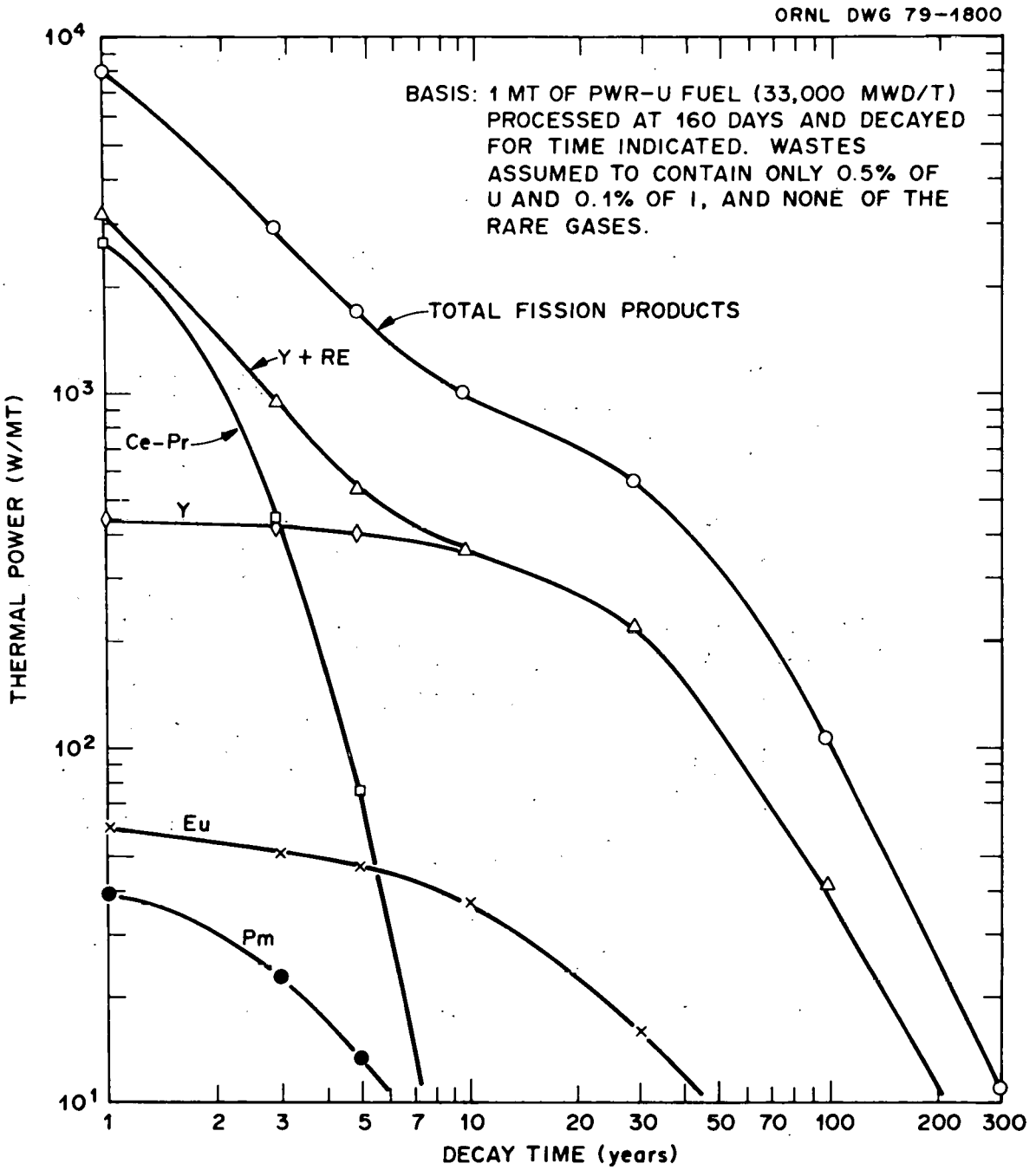

Fig. 1. Thermal power of HLW from conventional reprocessing of LWR fuel. Source: W. D. Bond and R. E. Leuze, *Feasibility Studies of the Partitioning of Commercial High-Level Waste Generated in Spent Fuel Reprocessing: Annual Progress Report FY-1974*, ORNL-5012 (January 1975).

ORNL DWG 78-4994

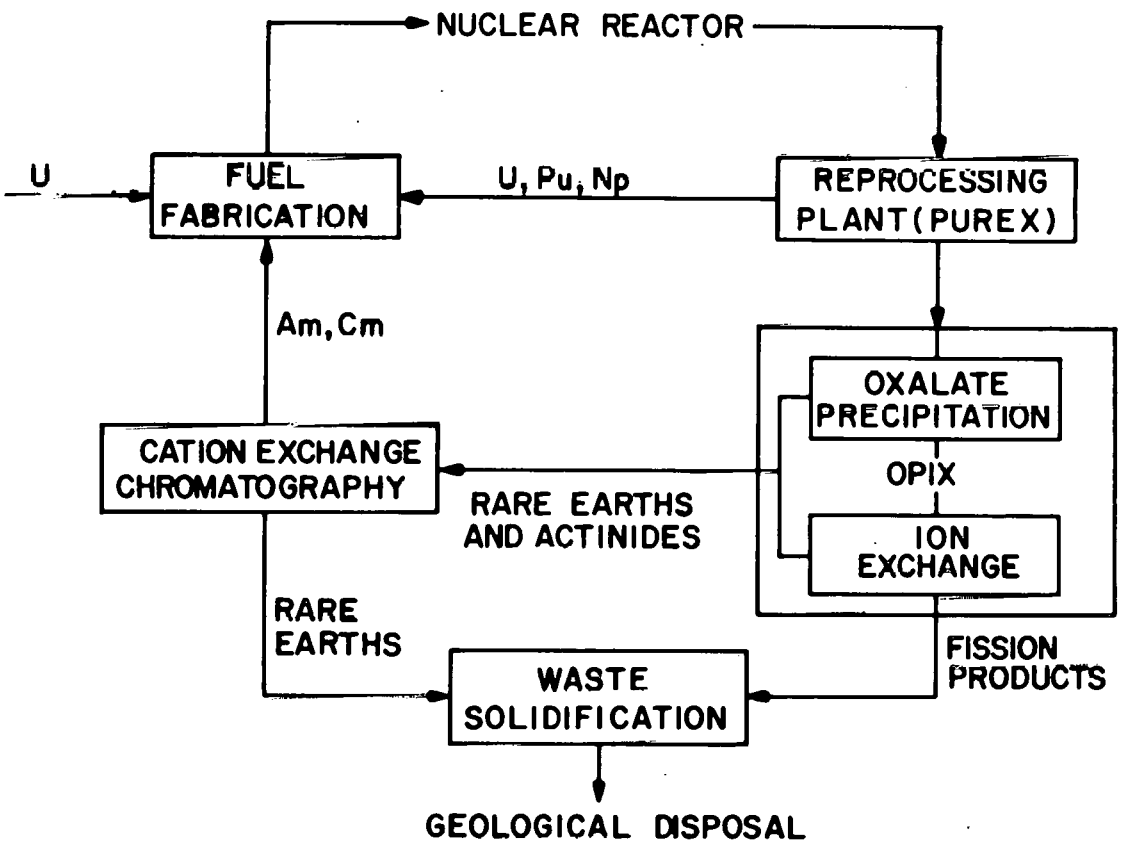

Fig. 2. Partitioning-transmutation flowsheet.

higher actinides are rejected to the HLW. Chemical feasibility studies[1-4] indicate that perhaps as much as 99.99% of the uranium and plutonium and 95% of the neptunium may be recovered in a modified Purex process. The HLW from the Purex plant contains essentially all of the americium, curium, and higher actinides. The OPIX process[5-7] is a candidate for use in the recovery of americium and curium from this waste. The OPIX process will separate the trivalent actinides and lanthanide elements from the other elements present in the HLW and will eliminate certain fission product elements, such as zirconium, which would interfere in the subsequent cation exchange chromatographic (CEC) process that is used to separate lanthanide from trivalent actinide elements. Chemical feasibility studies[1-4] have indicated that it may also be possible to recover 99.9% of the americium and curium.

A conceptual materials balance flowsheet for the OPIX process is shown in Fig. 3. The process consists of the following four basic operations:

1. precipitation of trivalent lanthanide and actinide oxalates with oxalic acid,
2. separation of a concentrated slurry of the oxalates from the mother liquor,
3. recovery of any residual actinides and lanthanides from the mother liquor using cation exchange resin, and
4. conversions of the oxalate slurry and the ion exchange product to solutions of nitrate salts in 0.5 M HNO_3, which can then be used as feed solutions to the CEC process.

Only the first two operations were investigated in this study.

The chemical feasibility of removing trivalent actinides and lanthanides by the OPIX process has already been demonstrated in batch laboratory-scale experiments with synthetic solutions and with real waste solutions.[5-7] Using very small samples of irradiated LWR fuel, D. O. Campbell showed that good recoveries are obtained in the oxalate precipitation step (Table 1). The OPIX process requires considerably less ion exchange resin than an all ion exchange process.[4] In addition to the ion exchange equivalents which are eliminated by the precipitation

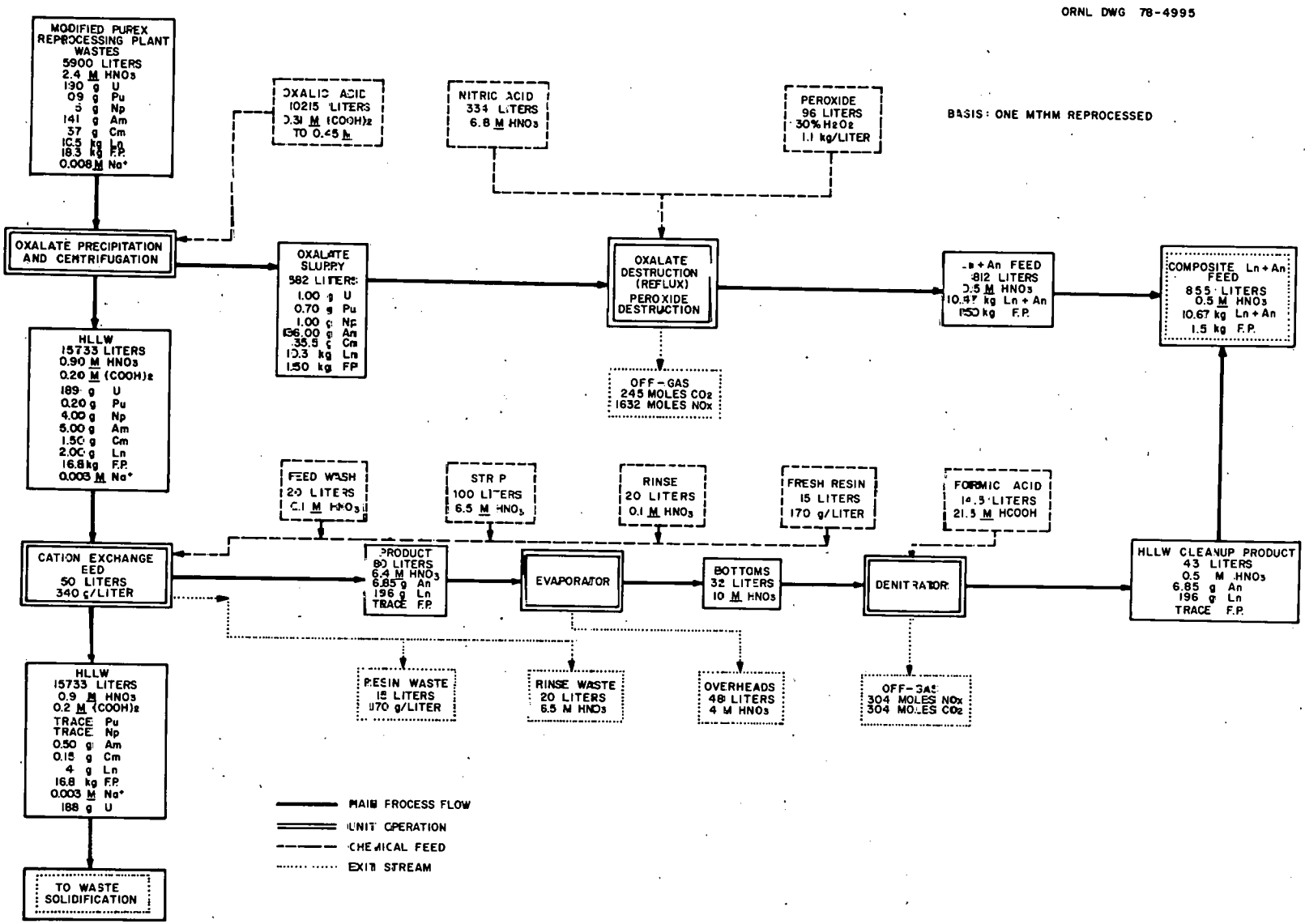

Fig. 3. Oxalate precipitation followed by ion exchange (OPIX) for trivalent actinides removed from HLW.

of the lanthanides and actinides, elements such as zirconium are strongly complexed by oxalate and are poorly sorbed by the cation resin. Oxalate precipitation not only reduces the amount of resin required but also reduces the amount of resin damaged by radiation.

Table 1. Hot cell results of actinide-lanthanide precipitation by oxalic acid[a]

Element	Percent in liquor	Percent precipitated
^{242}Cm	0.42	94.4
^{244}Cm	0.38	94.1
^{137}Cs	94.3	0.09
^{106}Ru	93.9	0.99
^{144}Ce	2.73	89.0

[a]High yields were difficult to measure; accuracy of yields may be ±30%.

3. EXPERIMENTAL

3.1 Precipitation and Crystallization Equipment

A stirred-tank reactor (STR) was used to carry out the precipitation and the subsequent growth of crystals. Industrial-type precipitator-crystallizers[8] were considered but were rejected because:

1. In industrial crystallizers, residence time of crystals (and hence crystal growth) is controlled by suspending the crystals in supersaturated liquid upflow through an increasing diameter tube. The linear, liquid velocity profile in the vertical tube is adjusted so that the large crystals settle out in the smallest diameter (highest linear velocity) section at the bottom of the tube, whereas the smaller particles remain suspended in the upper portions of the tube until sufficient crystal growth has been achieved. The author deemed this type of apparatus unsuitable in high radiation fields because gaseous CO_2 produced by the radiation is estimated to cause convective currents and make the operation of such devices questionable.

2. Heat and mass transfer are expected to be slow in such a crystallization arrangement and would require a longer residence time than in a stirred system. The longer residence time would permit greater quantities of oxalate ions to be decomposed by radiation.

Stirred-tank reactors have an additional advantage in that a considerable amount of literature is available on ways to scale up small equipment to large equipment. Several STRs may be operated in series.

The STR vessels and the impellers used in this study are shown in Fig. 4. The tanks contained four baffles each, and impellers were six-bladed. The ratios of vessel height and diameter were chosen to correspond to those reported in the literature[9-18] so that scale-up using known methods can be carried out if desired. If mass transfer is assumed to control system performance, geometrically equivalent scale-up to larger equipment having the same power input per unit volume of liquid should yield identical results. Although the maximum volume of the tanks was approximately 1.6 liters, precipitations were always carried out with the tanks filled to the 1-liter mark.

ORNL DWG 78-5108R2

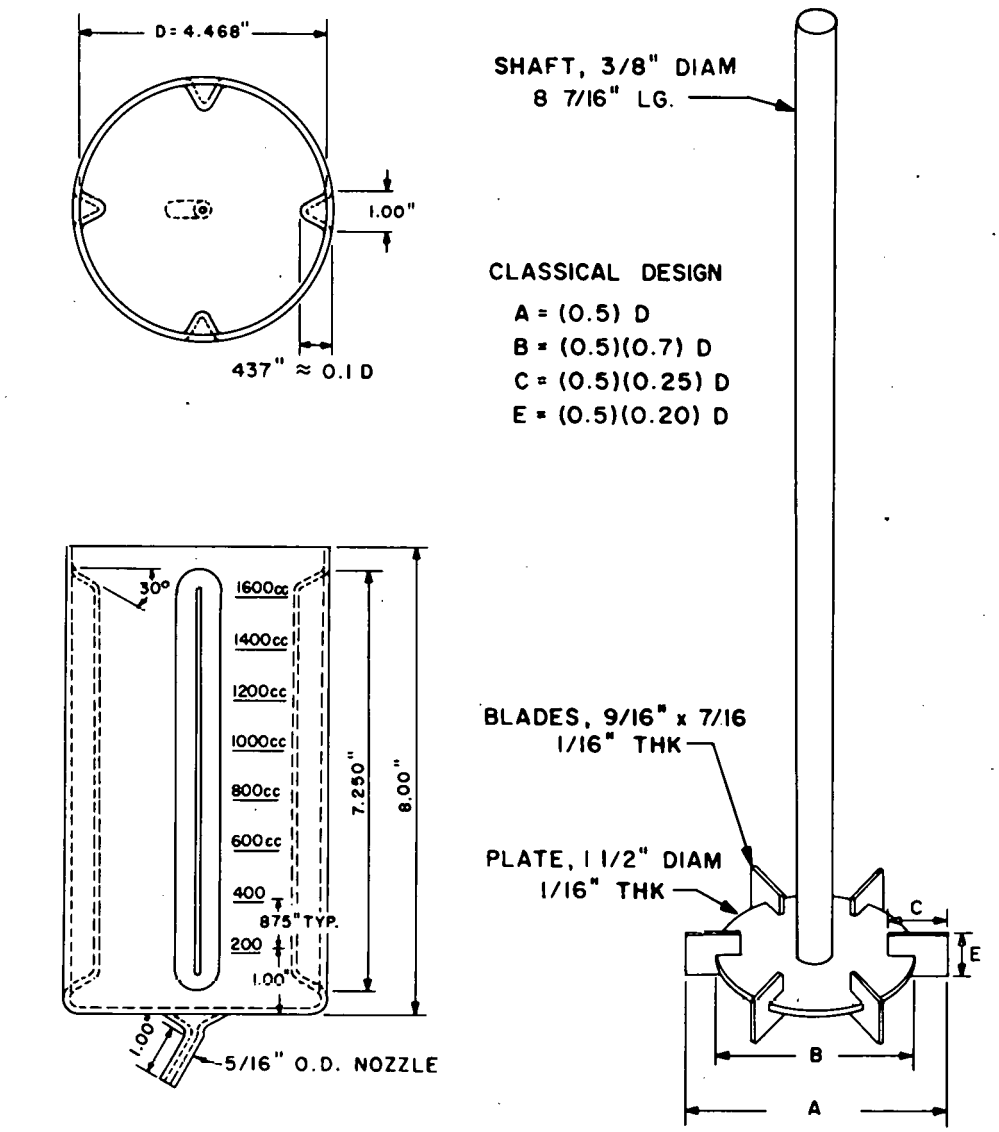

Fig. 4. Stirring impeller and STR.

3.2 Solid-Liquid Separations

Solid-liquid separations were investigated by both gravity settling and filtration.

3.2.1 Settler

A settler with a conical-shaped bottom was used to collect solids (Fig. 5). The slurry entered the settler near its midpoint, and liquid was separated by overflow. The cross section of the settler could be changed by placing various-sized glass rods in the middle of the settler. Although the settler was wrapped with insulating material, thermal convection still caused some difficulty. The problem was somewhat alleviated, though not eliminated, by heating the top of the settler with a heat lamp and by air cooling the bottom section of the settler. This created a thermal gradient of about 8°C between the bottom and top of the settler.

3.2.2 Filtration

Solid-liquid separations by filtration were tested with the use of three nucleopore filters in series (12, 5, and 1 μm pore diam). The amount of precipitate on each filter was measured. Filtration experiments were carried out after settling tests were completed. About 50 to 100 ml of slurry from the last STR was diverted to the series of filters.

Although the nucleopore filters are unsuitable for filtration of highly radioactive solids, they were used in this study for convenience. If filtration is to be used for highly radioactive solids, etched disk filters[9] should be substituted because they can be thermally cooled and can be made of any desired material. These filters, which are used at nuclear power stations, are currently available in pore diameters of 5 and 12 μm.

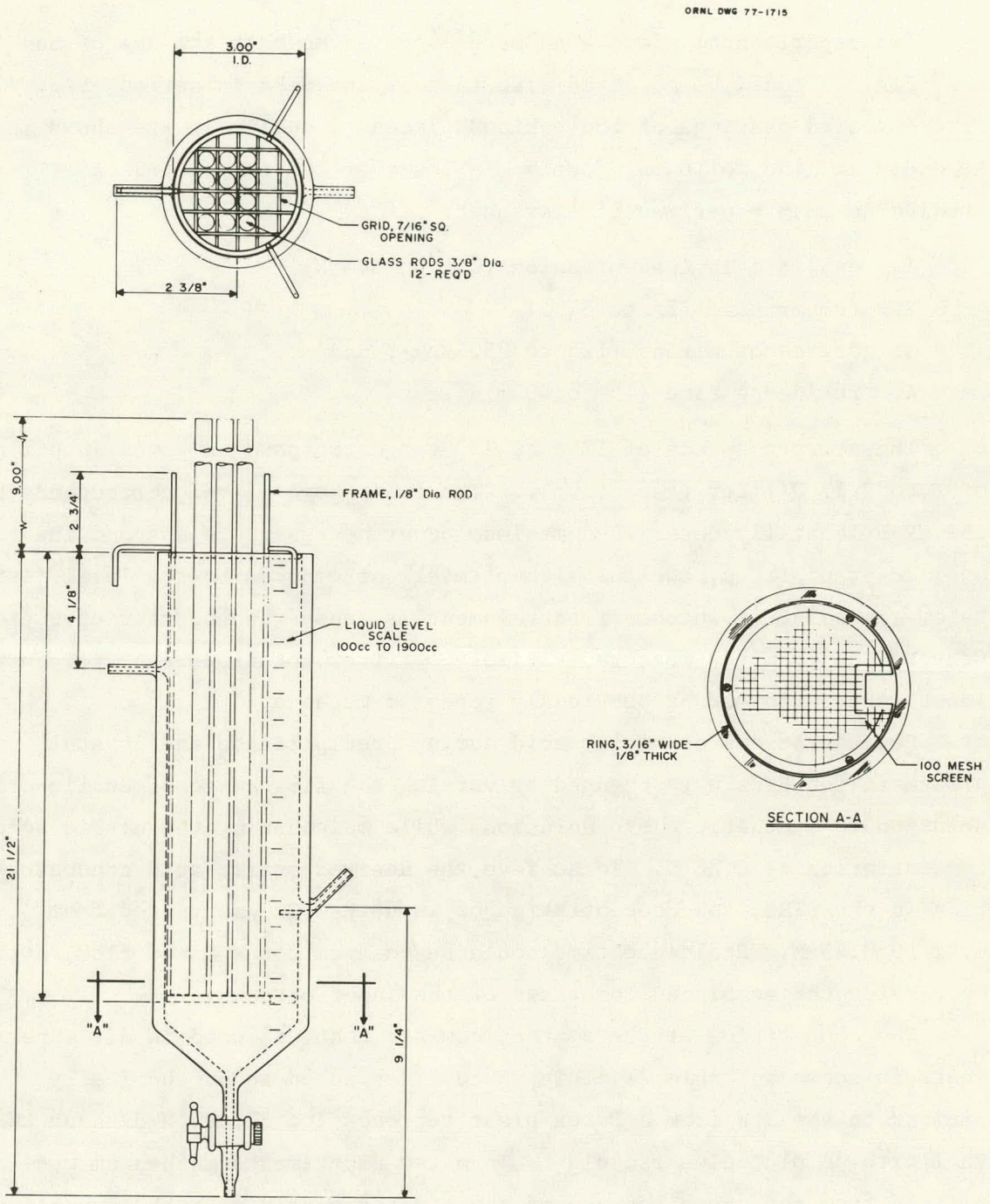

Fig. 5. Gravity settler.

3.3 Experimental Flowsheet and Process Parameters

Two experimental flowsheets were employed so that the use of one STR (Fig. 6) could be compared with that of two STRs in series (Fig. 7). More detailed drawings of the various pieces of equipment are shown in Appendix A. The following four variables over the ranges indicated were studied in each experimental flowsheet:

1. oxalic acid concentration (0.2 to 0.3 M),
2. temperature (25 to 50°C),
3. degree of mixing (125 to 250 rpm), and
4. residence time (15 to 40 min).

The stirrer speeds of 125 and 250 rpm correspond to power inputs of 0.02 to 0.17 W/liter respectively. The lower power level corresponds to the experimentally determined minimum power necessary to suspend the oxalate precipitate, and the higher level corresponds to the level just below the point at which air entrainment is caused by the stirrer action. Conversions from the measured variable, stirrer rotation rate, to power input were performed by previously reported methods.[10-19]

Concentrations of oxalic acid during precipitation and crystal growth in the STRs were changed by varying the flow ratio of oxalic acid solution to synthetic waste solutions while maintaining the nitric acid concentration at 0.88 M. To achieve the desired oxalic acid concentration in the STRs, the concentration of input $H_2C_2O_4$ was varied from 0.31 to 0.45 M. Residence time could be changed for a fixed flow ratio by varying the combined flow rates of the input streams.

The composition of the synthetic waste that was used in all experiments is shown in Table 2. This waste is expected to be chemically similar to the HLW from a Purex plant reprocessing 30,000 MWd/tonne LWR fuel with no plutonium recycle.[3] In a few experiments ruthenium was omitted from the waste because of the limited supply of ruthenium nitrate.

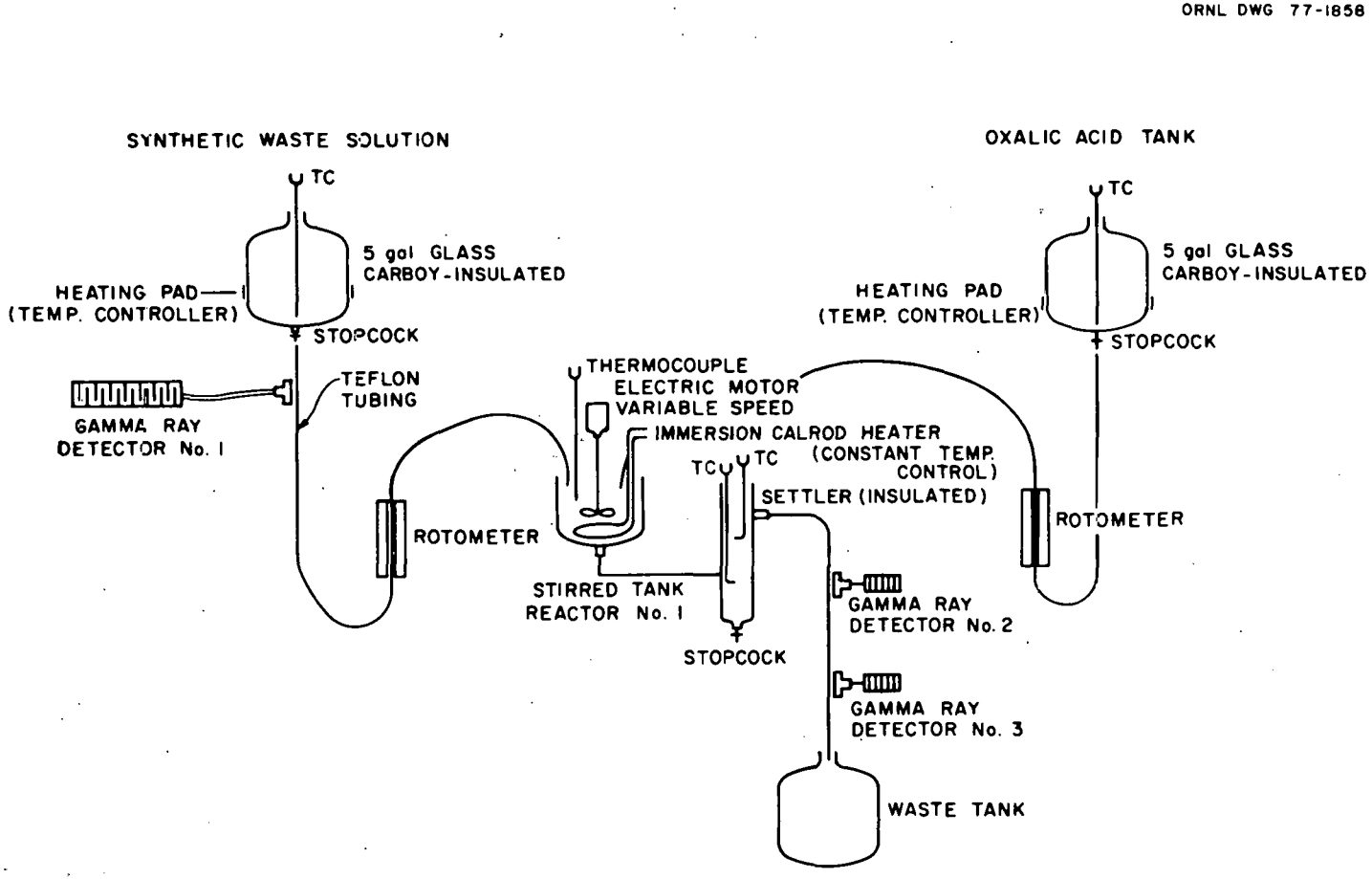

Fig. 6. Experimental equipment arrangement for experiments using a single STR.

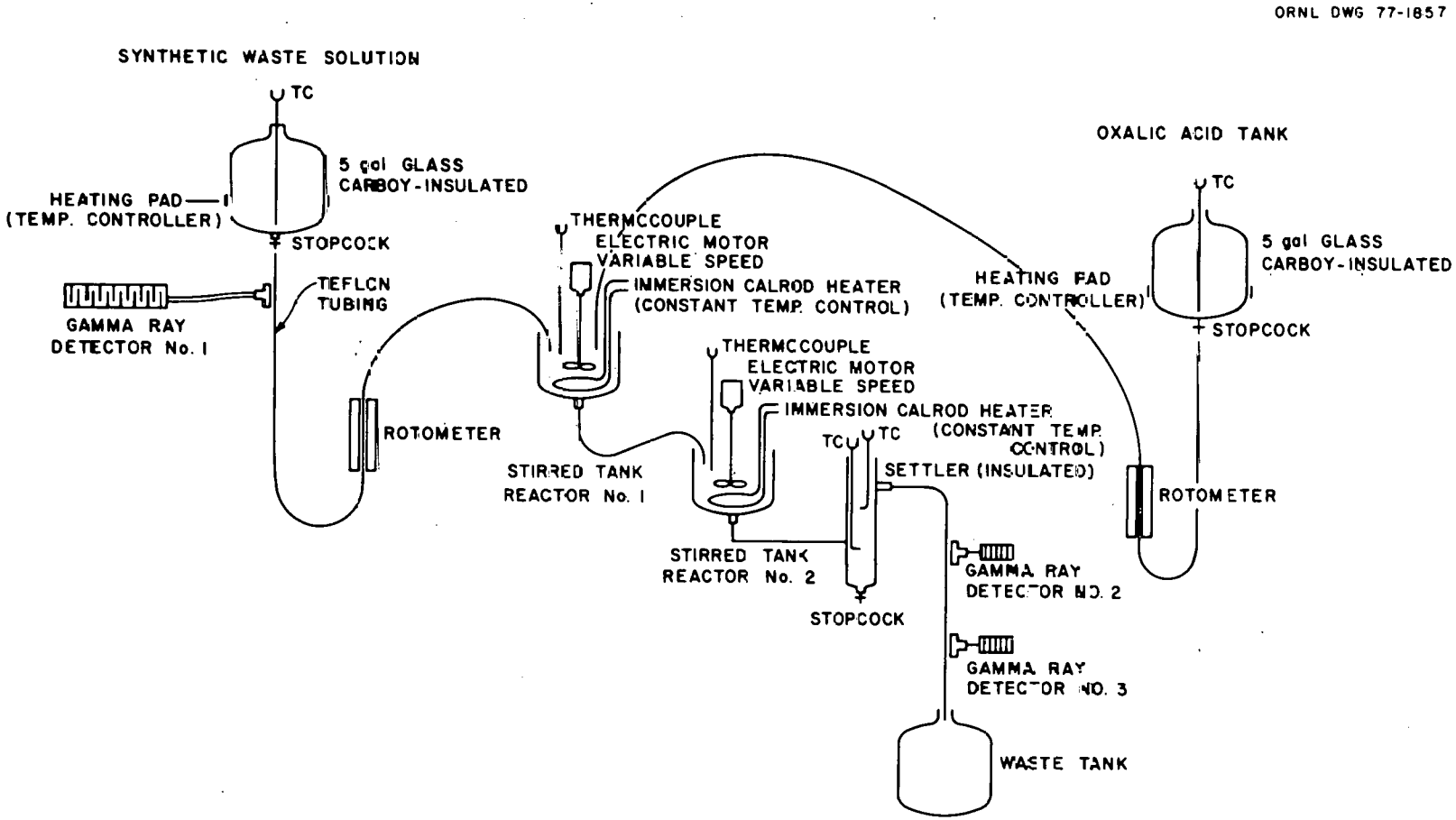

Fig. 7. Experimental equipment arrangement for experiments using two STRs in series.

Table 2. Synthetic waste solution composition

Element[a]	Amount (g/liter)
Lanthanides	
Lanthanum	0.205
Cerium	0.398
Praseodymium	0.196
Neodymium	0.660
Samarium	0.143
Europium	0.0275
Gadolinium	0.019
Dysprosium	0.0002
Holmium	0.000015
Erbium	0.000005
Group VIIIB	
Ruthenium	0.344
Rhodium	0.0625
Palladium	0.228
Group IA	
Rubidium	0.0535
Cesium	0.390
Group IIA	
Strontium	0.1315
Barium	0.268
Others	
Zirconium	0.585
Indium	0.0002
Yttrium	0.0755
Silver	0.0095
Cadmium	0.0185
Arsenic	0.000015
Antimony	0.002
Molybdenum	0.55
Selenium	0.008
Tellurium	0.0905
Tin	0.008

[a]Elements in solution of 2.5 M HNO_3.

Source: W. D. Bond and R. E. Leuze, *Feasibility Studies of the Partitioning of Commercial High-Level Waste Generated in Spent Fuel Reprocessing: Annual Progress Report FY-1974*, ORNL-5012 (January 1975).

3.4 Analytical Determination of Precipitate Yield

The yield of trivalent actinides and lanthanides in the oxalate precipitate was estimated by measuring the concentration of ^{142}Pr in the input and output liquid streams of the process. Because praseodymium oxalate is slightly more soluble than either americium and curium oxalates, it should give conservative estimates of the yields of americium and curium. Furthermore, ^{142}Pr ($t_{\frac{1}{2}}$ = 19.2 hr, 1.6-MeV γ) is a very convenient tracer isotope. When steady-state conditions had been reached (as indicated by an on-line gamma ray detector used to monitor the input feed stream and output clarified liquor streams), 5-ml samples of the input and output streams were withdrawn and counted using a Searle automatic gamma counter (Model 1185) to obtain highly accurate counting data.

3.5 Chemical Analyses of Precipitates and Supernatant Liquids

Samples were analyzed by spark source mass spectrometry by the Analytical Chemistry Division. The relative amounts of each element present were determined as abundance ratios. The abundance ratio is defined as the ratio of the mass of any given element X to the mass of any conveniently chosen standard element. The standard element may be a normal constituent of the sample or it may be deliberately added in known quantity. The abundance ratio of the standard element is unity by definition. In this study, praseodymium and barium were chosen as the the standard elements for abundance ratio determinations of the various elements in precipitate and liquid samples respectively. Since these elements were already present in the synthetic waste, percentages of any given element that precipitated or that remained in solution with respect to the standard element could be estimated by the following equation:

$$\text{percent yield of element } X = \frac{AR_{xs}}{AR_{xw}} \times 100 \ , \qquad (1)$$

where AR_{xs} and AR_{xw} are the abundance ratios of element X in the test sample and in the original synthetic waste solution respectively. Because

barium and praseodymium are standard elements, their percent yield calculated by Eq. (1) is always 100%. Corrected values for percent yield of an element could be calculated by multiplying the value obtained from Eq. (1) by the measured yield of the reference element (praseodymium or barium). The abundance ratios of the various elements in the original synthetic waste solution were determined each time a new set of experimental samples of precipitates and liquids were tested. This procedure minimized errors in analytical procedure and served as a check on instrument calibration.

Praseodymium was chosen as the standard element for precipitate samples because a high percentage was expected to precipitate in the experimental runs and because its yield was also being determined by the ^{142}Pr tracer method (Sect. 2.4). Barium was chosen as the standard for liquid samples because very little was expected to precipitate. In addition, barium and praseodymium are two of the more abundant elements in synthetic waste (Table 2) and hence are detected readily.

4. EXPERIMENTAL RESULTS AND ANALYSIS OF DATA

The experimental results were analyzed using a factorial method and a linear regression method. In these analyses, an attempt was made to numerically correlate the yield of oxalate precipitate to the statistically significant process variables. Correlations obtained from the numerical methods were, in most cases, in general agreement with conclusions that could be drawn by visual inspection of the raw data.

4.1 Experimental Results

The product yields obtained under different chemical and operational conditions are shown in Table 3 for precipitations carried out using a single STR and in Table 4 for two STRs in series. It is apparent from the data that yield is greater with the use of two STRs in series than with a single STR. Filtration was clearly superior to the gravity settler for separating the precipitate from the supernatant liquid. No attempt was made to determine if filtrates contained particles of precipitate that were less than 1 μm in diameter. The specific effects of the other variables are not quite as apparent as the use of one STR versus two in series. In general, increasing the oxalic acid concentration or the residence time increased the product yield, whereas increasing the temperature decreased product yield. These effects were expected because of mass action considerations and because lanthanide oxalate solubilities are known to increase with temperature. However, the improved yield with lower temperatures is contrary to what could be expected on the basis of mass transfer effects alone. Although effects of changes in mixing power cannot be clearly ascertained from the raw data, yields were generally increased by using either the longer residence times and the lower mixing powers or by using the higher mixing powers at any of the residence times tested.

The highest and lowest yields of precipitate obtained in runs with two STRs in series are given in Table 5. These results support our qualitative observations about the effects of variables in that the best yields occurred at the highest oxalic acid concentrations, highest mixing

Table 3. Experimental conditions and product yields for the continuous precipitation of rare earth oxalates using one STR

Experiment number	Liquid residence time per reactor (min)	Reactor temperature (°C)	Oxalic acid concentration in STR (M)	Mixing power (W/liter)	Product yield (%)			
					Settler	12-μm filter	5-μm filter	1-μm filter
A-15	16.0	27.3	0.21	1.61×10^{-2}	15.2	30.7	66.1	76.1
A-16	36.1	27.2	0.22	1.91×10^{-1}	77.4	77.9	80.1	82.6
A-17	36.1	52.4	0.22	2.33×10^{-2}	48.7	38.7	47.8	57.0
A-18	16.0	52.3	0.21	1.54×10^{-1}	40.0	36.2	44.9	50.0
A-19	34.7	27.3	0.32	2.73×10^{-2}	77.3	77.3	85.2	88.0
A-20	16.2	27.3	0.30	1.80×10^{-1}	78.4	78.2	83.9	88.2
A-21	16.2	52.3	0.30	2.12×10^{-2}	47.3	35.5	39.0	45.0
A-22	34.7	55.2	0.32	1.48×10^{-1}	64.8	76.7	78.5	86.2
A-23	25.7	39.9	0.26	6.94×10^{-2}	66.7	76.0	80.5	84.7
A-24	25.7	39.9	0.26	6.66×10^{-2}	80.9	76.5	81.2	84.9

Table 4. Experimental conditions and product yields for the continuous precipitation of rare earth oxalates using two STRs in series

Experiment number	Operating conditions					Product yield (%)						
						STR No. 1			STR No. 2			
	Liquid residence time per reactor (min)	Reactor temperature (°C)	Oxalic acid concentration in STR (M)	Mixing power of STR No. 1 (W/liter)	Mixing power of STR No. 2 (W/liter)	12-μm filter	5-μm filter	1-μm filter	12-μm filter	5-μm filter	1-μm filter	Settler
B-27	19.9	36.4	0.20	1.83×10^{-2}	2.17×10^{-2}	41.2	57.7	78.2	58.8	65.8	71.1	46.2
B-28	40.1	36.2	0.20	2.02×10^{-1}	2.38×10^{-2}	70.1	72.6	77.0	81.9	83.1	84.3	77.7
B-29	40.1	35.3	0.20	2.44×10^{-2}	1.68×10^{-1}	61.9	70.8	75.9	84.1	84.6	87.5	76.3
B-30	19.9	36.3	0.20	1.93×10^{-1}	1.84×10^{-1}	40.6	54.5	64.7	74.4	78.4	81.6	62.5
B-31	39.0	35.3	0.29	2.12×10^{-2}	2.61×10^{-2}	71.3	75.9	79.7	90.8	91.1	92.2	85.1
B-32	20.0	35.9	0.29	1.32×10^{-1}	1.97×10^{-2}	65.9	64.1	72.2	75.8	78.2	77.9	68.7
B-33	20.0	36.0	0.29	2.28×10^{-2}	1.74×10^{-1}	68.9	80.2	86.9	86.7	88.9	91.3	81.8
B-34	39.0	34.7	0.29	1.78×10^{-1}	1.58×10^{-1}	77.7	80.2	85.8	89.5	91.3	91.7	84.0
B-35	29.5	35.7	0.245	5.40×10^{-2}	6.61×10^{-2}	69.6	73.6	82.0	86.0	88.0	89.1	79.3
B-36	29.5	35.5	0.245	7.16×10^{-2}	6.61×10^{-2}	71.9	75.7	79.3	88.5	88.6	90.2	82.6
B-37	29.5	35.1	0.245	7.39×10^{-2}	7.27×10^{-2}	67.8	74.3	81.8	86.5	87.1	88.4	79.7

Table 5. Experimental conditions at which the highest and lowest yields of precipitate were obtained using two STRs in series

	Highest yield	Lowest yield
Experimental conditions		
Residence time per reactor, min	39.0	19.9
Mixing power, W/liter		
STR No. 1	1.78×10^{-1}	1.88×10^{-2}
STR No. 2	1.58×10^{-1}	2.17×10^{-2}
Temperature, °C	34.7	36.4
Oxalic acid concentration, M	0.29	0.20
Product yield, %		
Settler	84	46.2
Filtration		
12-μm filter	89.5	58.8
5-μm filter	91.3	65.8
1-μm filter	91.7	71.1

power inputs, and longest residence times. It seems clear from the raw data (Tables 3 and 4) that up to about 90% recovery of the lanthanide oxalates can be accomplished using two STRs in series. However, the high yields obtained with two STRs is in part an effect of residence time because total residence times were generally higher in the two-tank system. In an actual process, centrifugation would be the preferred method of separating the precipitate because a significant fraction of the precipitate particles (or agglomerates) are less than 12 μm in diameter.

Because these were the first experiments performed with continuous oxalate precipitation, additional work should result in more accurate results and a better understanding of process variables. A fully developed process should provide a high assurance of meeting separation goals without being unduly sensitive to process variables.

Elemental analyses of the oxalate precipitates and the supernatant liquids were made using the spark source mass spectrographic method (Sect. 3.5) in attempts to (1) establish the purity of the rare earth oxalate precipitate and (2) obtain a mass balance of fission products in the precipitation step. Results are shown in Tables 6 and 7. Precipitates were not washed prior to their analysis. The degree of precipitation of rare earths from the original slurries ranged from 50 to 85%. There were problems in analyzing liquid samples. Values obtained from liquid samples (Table 6) for elements other than the major rare earths were too high. For example, quantities of elements such as zirconium, molybdenum, and ruthenium were measured to be about 200% greater than in the original waste. All yield values obtained for trace elements (Table 7) in the precipitate (antimony, tin, indium, and minor rare earths) have large uncertainties associated with them. These uncertainties are larger than the measured standard deviation shown due to difficulties in equipment calibration for trace elements in the presence of bulk quantities of certain rare earths. For the unwashed precipitate, the following approximate amounts (percent of original waste solution basis) of contaminants are present:

Zr	5 to 8%
Ba, Sr, Ru, Cs, Pd	0.5 to 1.5%
Ru, Rh, Mo	0.1 to 0.5%

Table 6. Percentages of synthetic waste elements found in the oxalate precipitate and in the liquid phases of the single-STR system

Element	Precipitate from settler (%)[a]	Liquid associated with settler precipitate (%)[a]	Liquid from 1-μm filter system (%)[a]
Praseodymium	100.0[b]	10.31 ± 9.96	6.097 ± 2.494
Europium	108.4 ± 17.2	7.990 ± 4.119	26.62 ± 17.15[c]
Neodymium	113.3 ± 9.1	5.807 ± 2.188	5.402 ± 2.812
Barium	0.5925 ± 0.2698	100.0[b]	100.0[b]
Strontium	1.266 ± 0.703	106.7 ± 13.1	153.9 ± 16.5
Ruthenium	0.1350 ± 0.0469	149.5 ± 29.7	233.2 ± 58.0
Molybdenum	0.2375 ± 0.0948	141.7 ± 23.5	225.2 ± 56.4
Zirconium	5.203 ± 2.148	131.8 ± 32.1	229.0 ± 48.3

[a]Percentages are based on the total quantity of that element originally present in the synthetic waste (see Sect. 2.5). Percentage listed is the average of several measurements ± the standard deviation.

[b]Percentages are relative to praseodymium in the precipitate and barium in the liquid; that is, it is assumed that praseodymium precipitation is complete and that no barium precipitates.

[c]Only three samples rather than the usual eight samples.

Table 7. Chemical analysis of solid precipitate collected from experiments employing two STRs in series

Element	Percentage yields[a] (%)	Synthetic waste solution composition (g/liter)
Lanthanides		
Lanthanum	82.2 ± 4.8	0.205
Cerium	77.1 ± 15.6	0.398
Praseodymium[b]	100.0	0.193
Neodymium	111 ± 10	0.660
Samarium	258 ± 52	0.143
Europium	109 ± 28	0.0275
Gadolinium	346 ± 33	0.019
Dysprosium	424 ± 142	0.0002
Holmium	681 ± 327	0.000015
Group VIIIB		
Ruthenium	0.121 ± 0.008	0.344
Rhodium	0.394 ± 0.159	0.0625
Palladium	1.00 ± 0.33	0.228
Group IIA		
Strontium	1.21 ± 0.67	0.1315
Barium	0.614 ± 0.404	0.268
Group IA		
Rubidium	0.738 ± 0.161	0.0535
Cesium	0.563 ± 0.095	0.390
Others		
Tellurium	1.69 ± 0.74	0.0905
Antimony	6.56 ± 5.60	0.002
Tin	17.8 ± 9.6	0.008
Indium	35.1 ± 25.2	0.0002
Cadmium	1.43 ± 0.91	0.0135
Molybdenum	0.267 ± 0.090	0.550
Zirconium	7.77 ± 3.66	0.585
Yttrium	56.8 ± 14.8	0.0755

[a] Average ± the standard deviation of the percentage.

[b] By definition, the percentage yield of praseodymium is 100.0 (see Sect. 3.5) and the standard deviation is zero.

The yield of yttrium was high (~57%), but this was expected because yttrium is similar in precipitation behavior to the rare earth elements. Further work needs to be carried out using actual HLW solutions so that radiochemical methods can be used to accurately determine contaminants. Descriptions of the individual samples taken in this study and their analyses are given in Appendix B. Use of either 1 or 2 STRs resulted in no statistical differences in contaminant levels of precipitates obtained from experimental runs.

4.2 Factorial Analyses and Results

4.2.1 Description of method

The decision to investigate rare earth product yield as a function of four independent variables, two process systems, and four solid-liquid separation devices implies an extremely large number of experiments and large amounts of data. With limited resources, a statistically designed experiment to maximize information and minimize experimental work was absolutely necessary; therefore, a half-factorial statistical design was chosen.[20]

This type of experimental design assumes that over the range of variables to be investigated, the product yield Y can be written as follows for a system of four independent variables:

$$Y = \beta_0 + \beta_1 X_1 + \beta_2 X_2 + \beta_3 X_3 + \beta_4 X_4 + \beta_{1,2} X_1 X_2 + \beta_{1,3} X_1 X_3 + \beta_{1,4} X_1 X_4 + \beta_{2,3} X_2 X_3 + \beta_{2,4} X_2 X_4 + \beta_{3,4} X_3 X_4 + \beta_{1,2,3} X_1 X_2 X_3 + \beta_{1,2,4} X_1 X_2 X_4 + \beta_{1,3,4} X_1 X_3 X_4 + \beta_{2,3,4} X_2 X_3 X_4 + \beta_{1,2,3,4} X_1 X_2 X_3 X_4 , \quad (2)$$

where

β_i = constant to be determined,

$$X_i = \frac{\text{value of variable} - \text{midrange value of variable } i}{0.5 \times \text{range of variable } i} . \quad (3)$$

With this definition, X_i can vary from -1 to +1. For example, if temperature is to be investigated over the range 25 to 50°C, then

$$X_{temp} = \frac{V_i - 37.5°C}{12.5°C} ,$$

where V_i is the value of the variable; X_i is defined to simplify analysis of results. Because each X_i is allowed to vary over the same range of values, the β_i's are a direct measure of the importance of any single variable compared to any other variables. The values of β allow direct comparison of the importance of any one variable to any other variable.

In a full-factorial experiment, the high and low value of each variable would be used in the experiments to determine product yield. Consequently, 16 experiments would be necessary to determine the values of the 16 coefficients in Eq. (2). The methodology can best be visualized with an experiment having three rather than four variables. For a three-variable system, eight regular experiments (as represented by the corners of the cube in Fig. 8) plus two or more centerpoint experiments would have to be conducted. The centerpoint experiments are designed to estimate the statistical accuracy of the entire set of experiments.

Because a full-factorial experiment implies such a large number of experiments, a half-factorial experiment was chosen. Here, only half the number of experiments are needed: eight for four variables and four for three variables, plus centerpoint experiments. Clearly, the values of 16 unknown β's cannot be determined experimentally with only eight experimental runs; however, if the eight runs are chosen carefully, the values of certain combinations of β's can be determined. For example, if the experiments for four variables are chosen similarly to those for three variables, as shown by the dots in Fig. 8, the following eight combinations of β's can be determined:

$$\beta_0 + \beta_{1,2,3,4}$$
$$2(\beta_1 + \beta_{2,3,4})$$
$$2(\beta_2 + \beta_{1,3,4})$$
$$2(\beta_3 + \beta_{1,2,4})$$
$$2(\beta_4 + \beta_{1,2,3})$$
$$2(\beta_{1,2} + \beta_{3,4})$$
$$2(\beta_{1,3} + \beta_{2,4})$$
$$2(\beta_{1,4} + \beta_{2,3})$$

It is here that the power of the factorial experiment is evident. For example, we can determine $2(\beta_1 + \beta_{2,3,4})$. The corresponding variables

ORNL DWG 78-5238

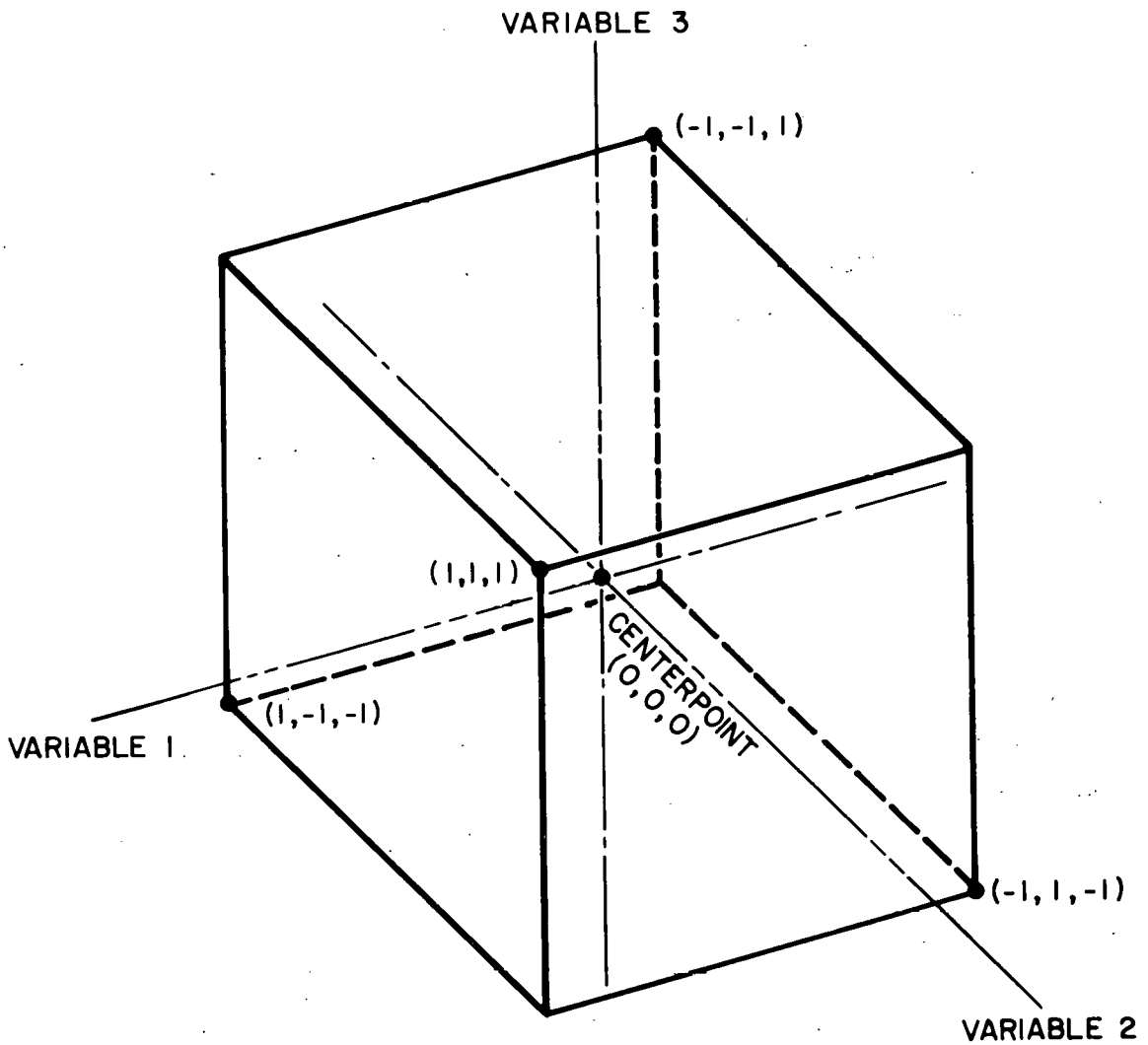

Fig. 8. Values of variables in factorial analysis.

for these β's are X_1 and $X_2X_3X_4$; however, X_1 and $X_2X_3X_4$ can only vary between -1 and +1. In any reasonably behaved system, it is extremely unlikely that the third-order cross term $\beta_{2,3,4}X_2X_3X_4$ is more important than the first-order term β_1X_1. It is reasonable, therefore, to assume that $2(\beta_1 + \beta_{2,3,4})$ is approximately equal to $2\beta_1$ and that $\beta_{2,3,4}$ is small compared to β_1. In effect, an estimate of β_1 free of second-order X_1 terms has been determined. Equally important, this estimate of β_1 estimates the effect of X_1 on product yields under a wide range of values of X_2, X_3, and X_4; that is, β_1 estimates average effects of X_1 on product yield over the range of all other variables investigated.

With this type of experiment, terms such as $2(\beta_{1,2} + \beta_{3,4})$ are more difficult to interpret. A low value could imply either that both terms are near zero or that one term is positive and the other is negative. In real systems, physical knowledge of the system can often show that either the X_1X_2 or X_3X_4 term is not physically realistic; hence, either $\beta_{1,2}$ or $\beta_{3,4}$ is zero.

4.2.2 Results of the factorial analyses

Tables 8, 9, and 10 report the experimentally determined values of β_i, error limits, definitions of X_i, and ranges of the variables for three systems and four solid-liquid separations per system. Table 8 lists the product yield values of β for the single-STR system. Table 9 shows values of β based on product yields from the first STR of the two-STR system, and Table 10 shows values from the second STR of the two-STR system.

The following experimental conclusions are evident from examination of the values of β_i in these tables:

1. Increased system temperature decreases product yield. In the single-STR experiments (Table 8), the system temperature was varied from 25 to 50°C. In all cases for all liquid-solid separation devices, the temperature coefficient of product yield, $2(\beta_2 + \beta_{1,3,4})$, is negative, implying that lower temperatures produce higher yields.

2. Increasing the amount of time the slurry spends in each STR improves product yield. In Table 10, which illustrates this point well,

Table 8. Values of β for single-STR system

Variable	Variable definition	Low value	High value
X_1 (V_1)	Time (min)	15	30
X_2 (V_2)	Temperature (°C)	25	50
X_3 (V_3)	Rotor speed (W/liter)	2.1×10^{-2}	1.7×10^{-1}
X_4 (V_4)	Oxalate concentration (M)	0.196	0.285

β (%)	Method of solid-liquid separation			
	Settling tank	12-μm filter	5-μm filter	1-μm filter
$\beta_0 + \beta_{1,2,3,4}$	56.1	56.4	65.7	71.6
$2(\beta_1 + \beta_{2,3,4})$	21.9	22.5	14.4	13.7
$2(\beta_2 + \beta_{1,3,4})$	-11.9	-19.3	-26.3	-24.2
$2(\beta_3 + \beta_{1,2,4})$	18.0	21.7	12.3	10.1
$2(\beta_4 + \beta_{1,2,3})$	21.6	21.1	11.9	10.5
$2(\beta_{1,2} + \beta_{3,4})$	-8.7	-0.6	6.8	10.6
$2(\beta_{1,3} + \beta_{2,4})$	-9.9	-2.4	0.5	1.7
$2(\beta_{1,4} + \beta_{2,3})$	-13.6	-2.4	6.0	6.8
90% confidence limit	±45.0	±1.4	±2.5	±0.8
95% confidence limit	±90.6	±7.8	±5.0	±1.5
99% confidence limit	±454.0	±14.3	±25.1	±7.7

Table 9. Values of β for first STR of two-STR system

Variable	Variable definition[a]	Low value	High value
X_1 (V_1)	Time (min)	20	40
X_2 (V_2)	Rotor speed STR No. 1 (W/liter)	2.1×10^{-2}	1.7×10^{-1}
X_3 (V_3)	Rotor speed STR No. 2 (W/liter)	2.1×10^{-2}	1.7×10^{-1}
X_4 (V_4)	Oxalate concentration (M)	0.196	0.285

β (%)	Method of solid-liquid separation		
	12-μm filter	5-μm filter	1-μm filter
$\beta_0 + \beta_{1,2,3,4}$	62.2	69.5	77.7
$2(\beta_1 + \beta_{2,3,4})$	16.1	10.8	4.4
$2(\beta_2 + \beta_{1,3,4})$	2.7	-3.3	-5.5
$2(\beta_3 + \beta_{1,2,4})$	0.2	3.8	1.8
$2(\beta_4 + \beta_{1,2,3})$	17.5	11.2	6.9
$2(\beta_{1,2} + \beta_{3,4})$	4.6	6.4	8.6
$2(\beta_{1,3} + \beta_{2,4})$	-1.0	-2.6	1.2
$2(\beta_{1,4} + \beta_{2,3})$	-9.0	-4.8	-1.1
90% confidence limit	±4.3	±2.2	±3.0
95% confidence limit	±6.3	±3.3	±4.5
99% confidence limit	±14.5	±7.5	±10.3

[a]All runs were conducted at ∿35°C.

Table 10. Values of β for second STR of two-STR system

Variable	Variable definition[a]	Low value	High value
X_1 (V_1)	Time (min)	20	40
X_2 (V_2)	Rotor speed STR No. 1 (W/liter)	2.1×10^{-2}	1.7×10^{-1}
X_3 (V_3)	Rotor speed STR No. 2 (W/liter)	2.1×10^{-2}	1.7×10^{-1}
X_4 (V_4)	Concentration $(COOH)_2$ (M)	0.196	0.285

β (%)	Method of solid-liquid separation			
	Settling tank	12-μm filter	5-μm filter	1-μm filter
$\beta_0 + \beta_{1,2,3,4}$	72.8	80.2	82.7	84.7
$2(\beta_1 + \beta_{2,3,4})$	16.0	12.7	9.7	8.5
$2(\beta_2 + \beta_{1,3,4})$	0.9	0.3	0.2	-1.7
$2(\beta_3 + \beta_{1,2,4})$	6.7	6.9	6.2	6.7
$2(\beta_4 + \beta_{1,2,3})$	14.2	10.9	9.4	7.1
$2(\beta_{1,2} + \beta_{3,4})$	-0.7	-2.1	-0.8	-0.2
$2(\beta_{1,3} + \beta_{2,4})$	-8.0	-6.4	-5.4	-5.3
$2(\beta_{1,4} + \beta_{2,3})$	-6.7	-3.7	-2.1	-1.1
90% confidence limit	±3.7	±2.7	±1.6	±1.9
95% confidence limit	±5.5	±4.0	±2.3	±2.8
99% confidence limit	±12.7	±9.2	±5.4	±6.4

[a]All runs were conducted at ∿35°C.

the reactor residence time coefficient, $2(\beta_1 + \beta_{2,3,4})$, varies from 16.0% for settler solid-liquid separation to 8.5% for 1-μm filter solid-liquid separation. This improvement in yield results from doubling the reactor residence time (from 20 to 40 min). The smaller improvement in product yield for the higher performance 1-μm filter is expected because after an initial crystallization period, longer residence times aid in growing larger crystals but do not significantly change the total weight of all precipitates in the slurry. The 1-μm filter catches most of the precipitate. The settler, however, requires longer times for larger crystals to form. Note that due to radiation damage considerations, it may not always be feasible to go to longer residence times.

3. In a two-tank system, the stirrer speed (power input) into the first STR does not significantly affect product yield. In Table 9, $2(\beta_2 + \beta_{1,3,4})$ estimates the importance of stirrer speed on product yield. At the 90% confidence level, the effect of stirrer speed on product yield varies from 2.7 ± 4.3% for the 12-μm filter to -5.5 ± 3.0% for the 1-μm filter. The statistical error limits are almost equal to the effect being analyzed, which implies that this variable does not statistically affect product yield within the range of values investigated.

4. Increasing the rotor speed (power input) for STR No. 2 improves product yield for the two-tank system. The factor $2(\beta_3 + \beta_{1,2,4})$ is a measure of the importance of stirrer speed. Increasing stirrer speed from 2.1×10^{-2} W/liter to 1.7×10^{-1} W/liter improves product yield by 6.7% for solid-liquid separation by both settler and 1-μm filter, as shown in Table 10 for the two-tank system.

5. Increasing oxalic acid feed concentration improves product yield as measured by the factor $2(\beta_4 + \beta_{1,2,3})$. For example, Table 10 shows a 14.2% product yield improvement for the settler and a 7.1% product yield improvement for the 1-μm filter when the oxalic acid feed concentration is increased from 0.3 to 0.45 M.

6. The settler is a poor solid-liquid separation device compared to filters. $\beta_0 + \beta_{1,2,3,4}$ is a measure of the average product yield under all operating conditions. This factor is consistently lower for settlers in all tables than comparable values for filters.

7. The settler performance was difficult to control. At the 90% confidence level in Table 8, the statistical uncertainty is measured at ±45.0% compared with 1.4% for the 12-μm filter. These statistical estimates were obtained by conducting identical experiments and measuring the product yields. If a piece of equipment is well behaved, duplicate runs yield basically duplicate results. Difficult-to-operate, difficult-to-control processes produce a wider variation in product yields. Because an equal number of duplicate runs were done for solid-liquid separation by both settler and filter, statistical uncertainty is usable as a measure of relative process controllability. These numbers provide experimental evidence against the use of continuous crystallizers in this system.

The values of various β terms can be combined into equations, but extreme care must be taken in their application. For example, let us consider an equation of product yield for the second STR of a two-STR system with a 12-μm filter. Let us assume that any value of β below the 95% confidence level is zero. Let us also assume that the system is reasonably well behaved; hence, third- and fourth-order interaction terms are zero. This leaves one problem term, $2(\beta_{1,3} + \beta_{2,4})$, where $\beta_{1,3}$ is an interaction term between reactor residence time and STR No. 2 rotor speed. Because this does not appear to be a likely interaction from physical considerations, it is set equal to zero. In contrast, $\beta_{2,4}$ is the interaction between rotor speed in the first STR and oxalic acid concentration. Higher oxalic acid concentration should nucleate more crystals with higher yields. High stirrer speeds, however, may improve local mass transfer, resulting in larger but fewer crystals. Because crystal growth rates depend on crystal surface area, a smaller number of larger crystals might result in lower crystal growth rates and hence in lower product yields. If we believe that this is physically realistic, then

$$Y = \beta_0 + \beta_1 X_1 + \beta_3 X_3 + \beta_4 X_4 + \beta_{2,4} X_2 X_4 \ . \qquad (4)$$

This type of equation is only applicable in the range of variables investigated and depends on the assumptions used to create it. Extreme care must be taken in using such equations because further experimental data are needed to confirm their validity.

4.3 Least Squares Analysis of Data

The data from the experiments using two STRs were also analyzed by a least squares technique in which the data were fitted to a linear equation of the form

$$Y = a_0 + a_1V_1 + a_2V_2 \ \ldots \ a_iV_i \ . \qquad (5)$$

Here, Y is the percent product yield, a_0 through a_i are constant coefficients, and V_1 through V_i are variables. Fifteen variables were considered, including reactor residence time, stirrer power to STR No. 1, stirrer power to STR No. 2, oxalic acid concentration, the cross products of these variables, the squares of these variables, and time (t) represented in the form e^{-t}. The data were analyzed using the SAS.76 computer program.[21] A description of the program and details of the data analysis are given in Appendix C.

The computer program fitted the data to all possible combinations of the above using one, two, three, and four variables at a time. The program then calculated the R^2 values for each equation obtained. (R^2 is a statistical concept that measures how well an equation represents the raw data and is commonly called the coefficient of correlation.[22]) The correlation coefficient ranges in value from 1.0 to 0, and no correlation is said to exist when $R^2 = 0$. A correlation among the variables, according to the test equation, is most probable when $R^2 = 1$. For example, a value of $R^2 = 0.88$ that is obtained using three sets of measured variables indicates that there is only a 12% chance of obtaining $R^2 = 0.88$ when no correlation exists. The probability of a true correlation increases for a fixed value of R^2 as the number of sets of experimental data is increased.[22]

Table 11 lists the three least squares equations which best represent product yield from the two-STR experiments with solid-liquid separation by a 12-μm filter. One observation is self-evident: product yield shows a primary dependence on e^{-t}.

Table 11. Least squares equations for product yields of experiments using the two-STR system and solid-liquid separation by 12-μm filter

Equation[a]	Value of R^2
One variable	
$Y = 61.284 + (2.883 \times CT)$	0.561
Two variables	
$Y = 59.513 - (6.0 \times 10^9 \times e^{-t}) + (112.009 \times COOH)$	0.759
Three variables	
$Y = 56.105 + (1.1631 \times 10^3 \times COOH) - (6.4938 \times 10^9 \times e^{-t}) + (2.4170 \times 10^2 \times W22)$	0.881

[a]Where Y = product yield, %; CT = oxalic acid concentration x time, moles·min/liter; t = time, min; COOH = oxalic acid concentration, moles/liter; $W22$ = power to STR No. 2 squared, $(W/liter)^2$.

4.4 General Observations

While planning, debugging, and conducting experiments, many semi-quantitative results were obtained. These include effect of certain elements on the rate of crystallization, operability of equipment, rate of plate-out of precipitate on equipment, and type of crystal formed. In addition, a few tests were run in an attempt to carry out oxalate precipitations using a homogeneous precipitation technique and to produce a more uniform particle size in the product. Attempts were made to utilize the hydrolysis reaction of diethyl oxalate to generate oxalate ion homogeneously. The results of the homogeneous precipitation tests were inconclusive and are reported in Appendix D.

4.4.1 Semicontinuous precipitation of rare earth oxalates

While the continuous precipitation equipment was being installed, a short series of semicontinuous precipitation experiments were carried out. The experiments attempted to duplicate a continuous process with a batch technique. For most experiments, a flask with a magnetic stirrer was filled with a 150-ml solution made of synthetic waste solution and oxalic acid. Every 10 min, a 15-ml sample was withdrawn, and the following solutions were added to the flask: (1) 10 ml of 0.3 M oxalic acid solution which also contained 0.15 M HNO_3 and (2) 5 ml of a synthetic waste solution containing 1.8 g/liter of rare earths, other fission products, and 2.4 M HNO_3. After six or seven samplings, the slurry in the flask began to come to steady state.

The samples taken were slurries of crystals and solution. A pipettor, a constant volume sampling device capable of taking fairly representative samples, was used for sampling. The samples were poured into 25-ml graduated cylinders, and the settling rate of the solid was measured as a function of time.

The results of these experiments, shown in Table 12, led to the following conclusions:

1. Strontium and barium interfere with the settling of rare earth precipitates. A series of identical runs were made using different types of synthetic waste solutions, as shown in Table 12. Wastes made of pure

Table 12. Influence of other fission product elements on the settling rates of precipitates of rare earth oxalates in batch precipitation tests

Run No.	Feed composition	Settling velocity (cm/min)[a]		
		From 15 to 13 cm^3 mark	From 13 to 11 cm^3 mark	From 11 to 9 cm^3 mark
1	Complete synthetic waste	0.733	1.808	0.685
2	Neodymium only, equivalent concentration	2.07	1.68	1.62
3	Zr only	No precipitate	No precipitate	No precipitate
4	Lanthanides + Ru	1.05	1.85	1.36
5	Lanthanides + Ru + Zr	1.59	1.91	1.72
6	Lanthanides + Ru + Zr + Ba	0.378	0.310	0.264
7	Lanthanides + Ru + Zr + Sr	0.294	0.264	0.353
8	Ba + Sr only	No precipitate	No precipitate	No precipitate

[a]Settling velocities were measured by following the clear-particulate interface as the particles settled in a graduated cylinder.

neodymium precipitated rapidly compared to full synthetic waste solutions. Additional experiments successively adding Ru, Zr, Ba, and Sr showed that barium and strontium caused the slower rate of settling. Pure barium and strontium do not precipitate in oxalic acid with the present experimental conditions. About 15 min was required to complete approximately 99% settling of synthetic waste solutions containing these two elements. It is believed that the presence of some barium and strontium interferes with rapid crystal growth.

2. Microscopic examination of the precipitate indicated that crystals, not agglomerates of crystals, are formed. The pure crystals are rods with a length to diameter ratio of 5 and a rod length of about 0.001 in. (2.5×10^{-3} cm). Many crystals are formed imperfectly with faulted crystal growth. In such cases, the crystal may appear spherical but upon close examination is shown to be a cluster of rod-like crystal projections that have grown from a central point.

3. The volume of the settled precipitate cake was less than 1% of the volume of the mother liquor.

4. The size of the precipitate indicates that settling and decantation may not be a workable method of solid-liquid separation. Several experiments were attempted at 40°C. The laboratory equipment was not insulated, and thermal convection caused by cooling of the graduated cylinder walls was sufficient to prevent settling of the precipitate. The higher levels of heating generated by radioactive decay in the precipitate may cause sufficient thermal convection to prevent separation. Either centrifuge or filters will likely be required for the solid-liquid separation.

5. The density of the precipitate is about 2.0 g/cm^3. This is calculated assuming a settling velocity of 0.75 cm/min, room temperature operation, spherical crystals with a diameter of 6.0×10^{-4} in. (1.5×10^{-1} cm), viscosity equal to water, and use of Stokes law. There is a great deal of uncertainty in this calculation.

The implications for future work are twofold:

1. Future experiments and equipment checkout before hot operation must use full synthetic waste solutions. Data and results of oxalate

precipitation equipment using rare earth solutions cannot be extrapolated to real waste solutions.

2. Oxalate precipitate settling rates depend on the amounts of barium and strontium in the waste solutions. Changing fuel types may change system behavior. For example, a BWR fueled with uranium produces about 4.44×10^{-2} g of barium per MWd and 2.7×10^{-2} g of strontium per MWd, compared to 4.15×10^{-2} g of barium per MWd and 1.59×10^{-2} g of strontium per MWd for an LMFBR. The difference in strontium levels is great enough for some difference in oxalate precipitation rates to be expected bewteen LWR and LMFBR fuels.

4.4.2 System operations

Experimentally, it was easier to maintain a uniform product removal rate with the two-STR system than with the single-STR system. Small variations in operating conditions quickly upset the single-tank system but did not upset the two-tank system. No quantitative measure of this was made.

4.4.3 Precipitate formation on equipment

During some experiments, oxalate precipitate formed on solid surfaces of the equipment in addition to forming as solids from solution. The following observations about this plate-out process were made:

1. Solids plated only onto stainless steel surfaces, not glass or Teflon.

2. In all cases the solids were easily removed by dissolution in 3 M nitric acid at room temperature.

3. In single-STR experiments, plate-out of material was observed in both the STR and the settler. In experiments where two STRs were employed in series, plate-out of material on equipment surfaces was only observed in STR No. 1. It is believed that plate-out of solids only occurs when the solution is highly supersaturated with oxalate ion; this supersaturation only occurs when the oxalic acid and waste solution are mixed together. The slightly longer residence time for STR No. 1 in the two-tank series limited oxalate plate-out to that STR.

4.4.4 Crystal form

Two typical photomicrographs of the solid precipitate are shown as Figs. 9 and 10. The solids in all cases were crystalline in nature. These photomicrographs cannot be used for accurate size measurement because 10 to 60 min elapsed between sampling and photography. In this time period, there can be significant crystal growth and dissolution.

ORNL-PHOTO 1701-78

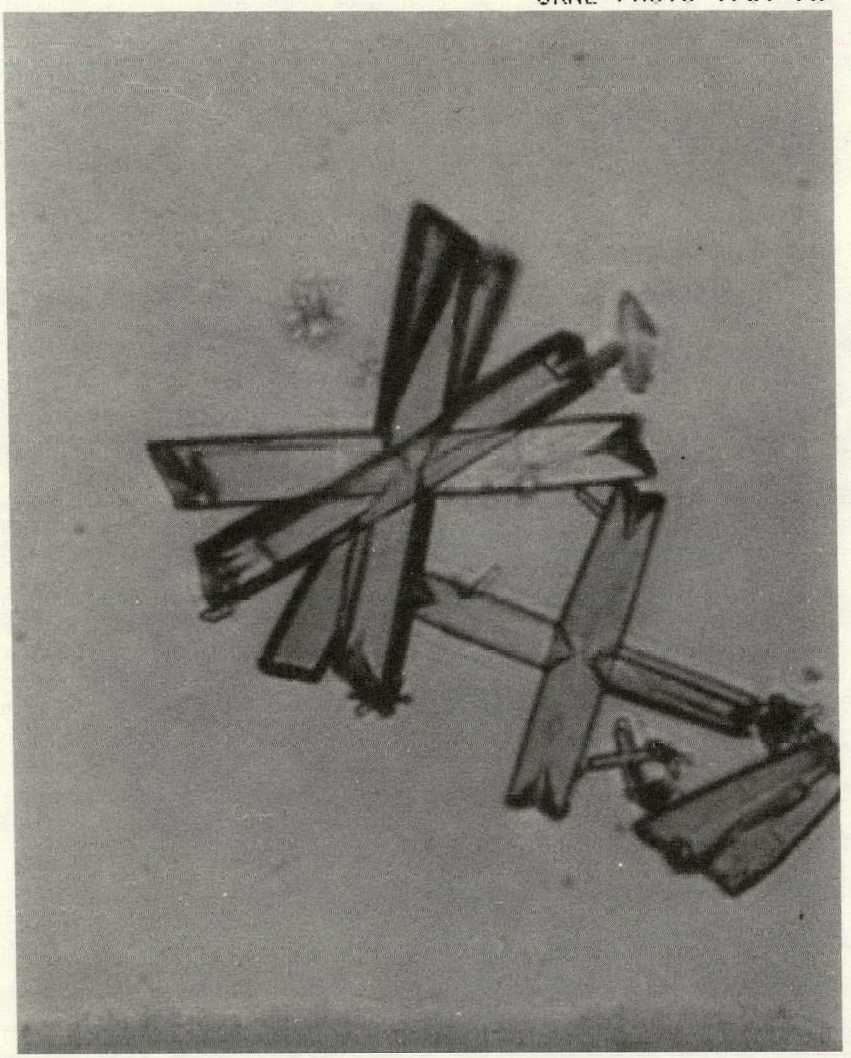

Fig. 9. Oxalate crystal.

ORNL-PHOTO 1700-78

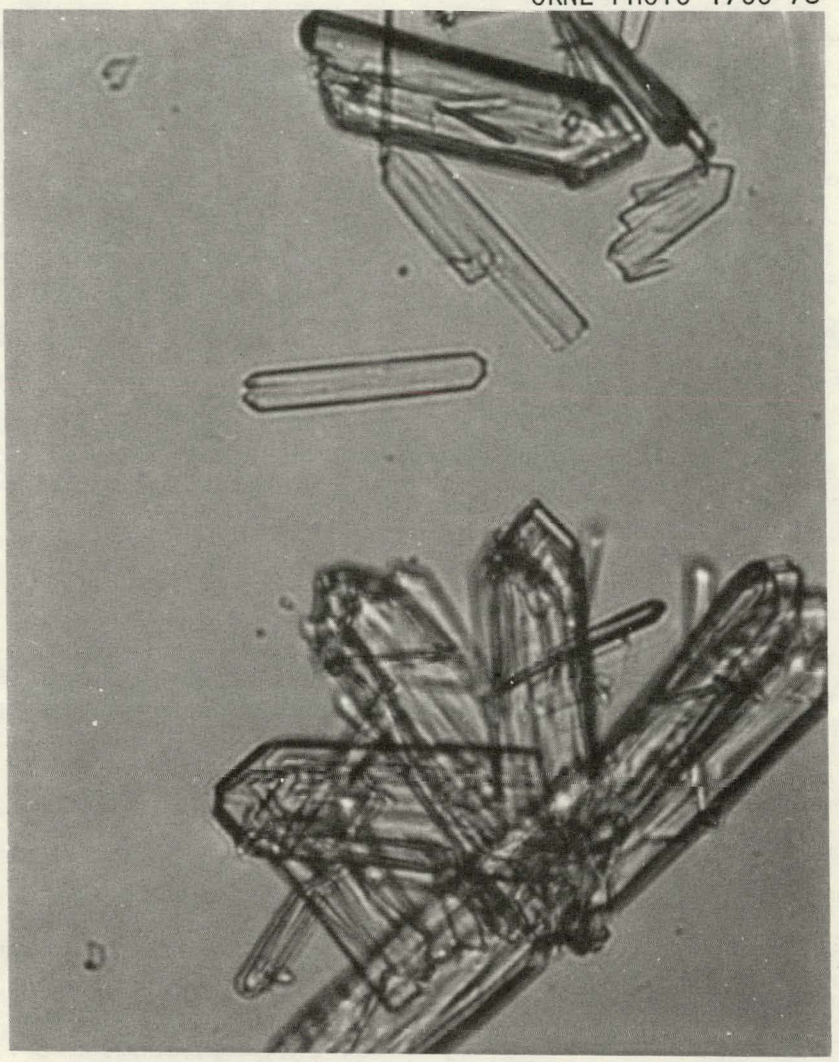

Fig. 10. Oxalate crystal.

5. CONCLUSIONS AND SUGGESTIONS FOR FUTURE WORK

The work to date indicates no fundamental problems using continuous oxalate precipitation to remove trivalent actinide and rare earth elements from HLW. This study shows that 90% yields of rare earth oxalates could be attained from synthetic waste solutions. It is expected that a somewhat greater (certainly no smaller) percentage of americium and curium would be precipitated along with the rare earths because of the mass action effect from the larger concentrations of rare earths in HLW. How high levels of radiation affect the process operability remains to be determined.

5.1 Effects of Process Variables

1. Yields of oxalate precipitate increased with increasing oxalic acid concentration and increasing residence time and decreased when the temperature was increased. Oxalic acid concentrations were varied from 0.2 to 0.3 M. Residence times were varied from 15 to 80 min, and temperatures were varied from 25 to 50°C.

2. Precipitations carried out using two STRs in series gave higher yields of precipitate than did the single-STR system. In addition, the performance of the series of two STRs was less affected by upsets in process operations (i.e., flow rate adjustments, minor fluctuations in temperature, etc.). However, the advantages of using two STRs in series are primarily evident when larger particles (12 μm diam) are filtered from the product slurry. Evidence for higher yield performance was based on statistical evidence rather than on direct comparisons at the same process conditions.

3. Stirrer speeds (i.e., mixing power) had no effect on product yield except in the second STR of the two-STR system. Statistical analyses indicate that the use of the highest stirrer speeds (250 rpm) in the second reactor gave slightly improved yields.

4. Separation of precipitates from mother liquors by filtration gave greater yields than by gravity settling. In the flowing system, it

was difficult to settle the oxalate precipitate because of the small particle sizes and the relatively low particle density.

5.2 Suggestions for Future Work

1. Results of this work indicate that the yield of oxalate precipitate begins to level off at a total residence time of 80 min. Experiments at greater residence times (e.g., 160 min) should be carried out to further confirm this observation.

2. Effects of changes in mixing power applied to impellers were difficult to interpret except by a statistical analysis. Additional work needs to be performed to better understand the effects of mixing.

3. A variable-speed continuous centrifuge should be tested for the separation of the oxalate precipitate from the liquid.

4. In some experiments, oxalate crystals plated onto equipment surfaces. The condition that promotes this behavior should be investigated for the purpose of either encouraging or eliminating it. If a material that encourages both growth and plate-out could be found, it might be used as a collection device for the precipitate. The collected precipitate could then be removed from the surface by acid dissolution.

5. Better characterization of the crystalline nature of the oxalate precipitate is needed. Because of the potential for crystal growth during the aging of samples, characterization must be completed within a few minutes after samples are taken.

6. Further studies to determine the purity of oxalate precipitates should be carried out. A procedure better than the one used in this study is necessary for determining the Zr, Mo, Ru, and noble metal impurities. Such studies may require the use of actual HLW solutions rather than synthetic solutions.

7. After completion of above items 1 through 6, experiments should be performed using actual, rather than synthetic, wastes. The effects of radiolytically generated CO_2 (from oxalic acid) on continuous precipitation performance would be evaluated in these tests. It should be pointed out, however, that batch-wise oxalate precipitation has been commonly employed[23] for the recovery of transplutonium elements at high radiation levels.

8. It must be determined experimentally that filtrate or centrifugate from the oxalate precipitation step can be treated satisfactorily by cation exchange to remove the residual actinides and rare earths.

6. REFERENCES

1. A. G. Croff, D. W. Tedder, J. P. Drago, J. O. Blomeke, and J. J. Perona, *A Preliminary Assessment of Partitioning and Transmutation as a Radioactive Waste Management Concept*, ORNL/TM-5805 (September 1977).
2. W. D. Bond, H. C. Claiborne, and R. E. Leuze, "Methods for Removal of Actinides from High-Level Wastes," *Nucl. Technol.* 24: 362 (1974).
3. W. D. Bond and R. E. Leuze, *Feasibility Studies of the Partitioning of Commercial High-Level Waste Generated in Spent Fuel Reprocessing: Annual Progress Report FY-1974*, ORNL-5012 (January 1975).
4. W. D. Bond and R. E. Leuze, "Removal of Actinides from High-Level Wastes Generated in the Reprocessing of Commercial Fuels," in *Transplutonium Elements*, W. Muller and R. Lindner, Eds., North-Holland, Amsterdam, 1976, pp. 423-31.
5. D. O. Campbell and S. R. Buxton, "Recovery of Transplutonium Elements from Nuclear Wastes," U.S. Patent 4,025,602 (May 24, 1977).
6. D. O. Campbell and S. R. Buxton, "Recovery of Americium and Curium from Nuclear Fuel Reprocessing Waste Solutions," abstracts of papers from American Chemical Society Annual Meeting, Aug. 29-Sept. 3, 1976, San Francisco, Calif.
7. *Chemical Technology Division Annual Progress Report for Period Ending March 31, 1975*, ORNL-5050 (1975), pp. 6-11, 30, 31.
8. M. A. Larson, "Guidelines for Selecting a Crystallizer," *Chem. Eng.* 85(2): 90 (1978).
9. T. Van den Berg and T. W. Lansey, "Backwashing a Stacked Disk Filter," *Trans. Am. Nucl. Soc.* 17: 322 (1973).
10. S. J. Khang and O. Levenspiel, "The Mixing-Rate Numbers for Agitator-Stirred Tanks," *Chem. Eng.* 83(10): 142 (1976).
11. R. W. Hicks, J. R. Morton, and J. G. Fenic, "How to Design Agitators for Desired Process Response," *Chem. Eng.* 83(4): 102 (1976).
12. R. L. Bates, P. L. Fondy, and R. R. Corpstein, "An Examination of Some Geometric Parameters of Impeller Power," *Ind. Eng. Chem. Process Des. Dev.* 2: 310 (1963).

13. D. S. Dickey and R. W. Hicks, "Fundamentals of Agitation," *Chem. Eng.* 83(2): 93 (1976).

14. F. P. O'Connell and D. E. Mack, "Simple Turbines in Fully Baffled Tanks," *Chem. Eng. Prog.* 46(7): 358 (1950).

15. L. E. Gates, J. R. Morton, and P. L. Fondy, "Selecting Agitation Systems to Suspend Solids in Liquids," *Chem. Eng.* 76(5): 144 (1976).

16. J. H. Rushton, E. W. Costich, and H. J. Everett, "Power Characteristics of Mixing Impellers, Part II," *Chem. Eng. Prog.* 46: 467 (1950).

17. C. M. Borgonovi, J. E. Hammelman, and C. L. Miller, "Dynamic Process Model of a Plutonium Oxalate Precipitator," *Trans. Am. Nucl. Soc.* 28: 374-75 (1978).

18. R. R. Rautzen, R. R. Corpstein, and D. S. Dickey, "How to Use Scale-Up Methods for Turbine Agitators," *Chem. Eng.* 83(10): 119 (1976).

19. D. S. Dickey and J. C. Fenic, "Dimensional Analysis for Fluid Agitation Systems," *Chem. Eng.* 83(1): 139 (1976).

20. T. D. Murphy, Jr., "Design and Analysis of Industrial Experiments," *Chem. Eng.* 84(6): 168 (1977).

21. A. J. Barr, J. H. Goodnight, J. T. Sall, and J. T. Helwig, *A Users Guide to SAS.76*, SAS Institute, Inc., Raleigh, N.C., 1976.

22. W. York, *Applied Statistics for Engineers*, 2d ed., McGraw-Hill, New York, 1969, pp. 267-68.

23. R. E. Leuze and M. H. Lloyd, "Processing Methods for the Recovery of Transplutonium Elements," in *Progress in Nuclear Energy Series III: Process Chemistry*, vol. 4, F. R. Bruce, J. M. Fletcher, and H. H. Hyman, Eds., Pergamon Press, New York, 1969, pp. 549-630.

24. J. A. Hermann, *Coprecipitation of Am(III) with Lanthanum Oxalate*, LA-2013 (March 1956).

Appendix A. EQUIPMENT DETAILS

THIS PAGE

WAS INTENTIONALLY

LEFT BLANK

Appendix A. EQUIPMENT DETAILS

This appendix contains more detailed drawings and photographs of the experimental equipment than those used in the text. The titles are self descriptive. Prior to photographing the equipment, some of the insulation and lead shielding for the detectors was removed to provide a better view.

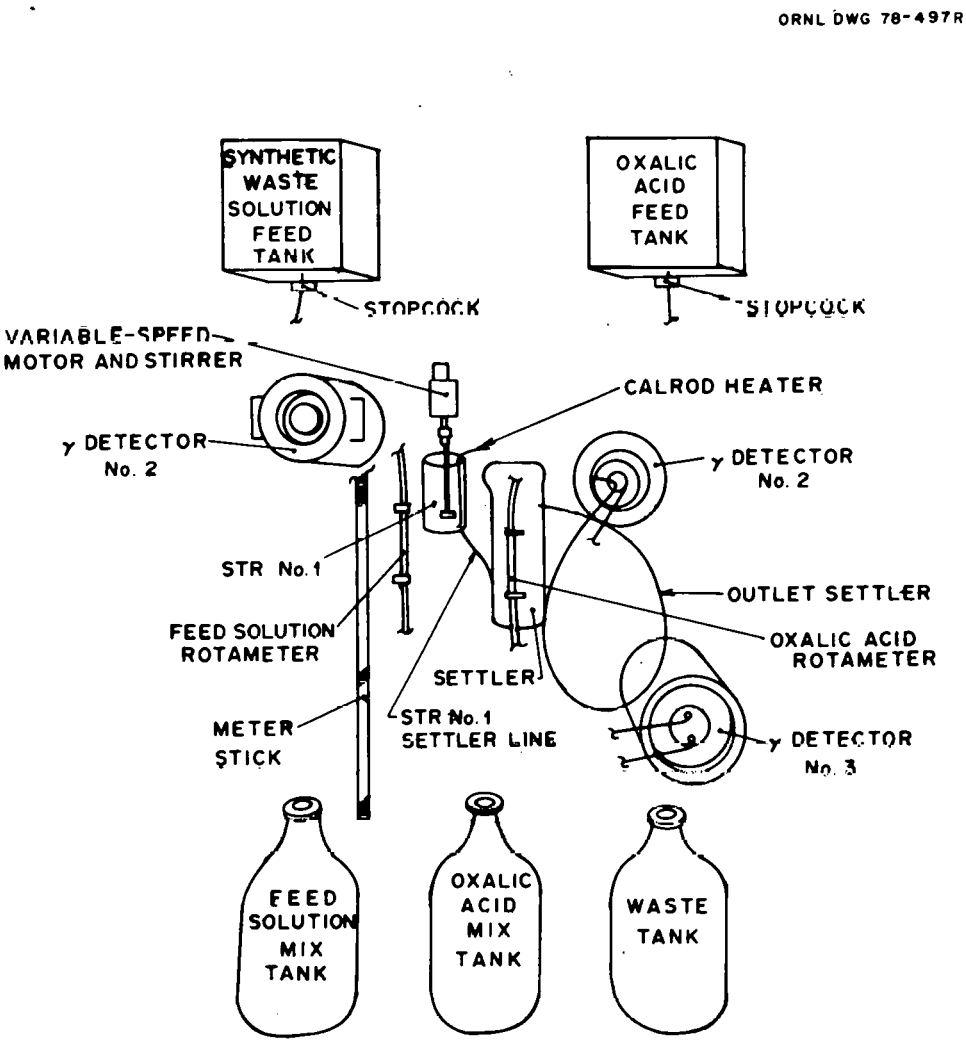

Fig. A.1. Components of experimental apparatus for single-STR experiments with continuous oxalate precipitation.

ORNL-PHOTO 3901-77

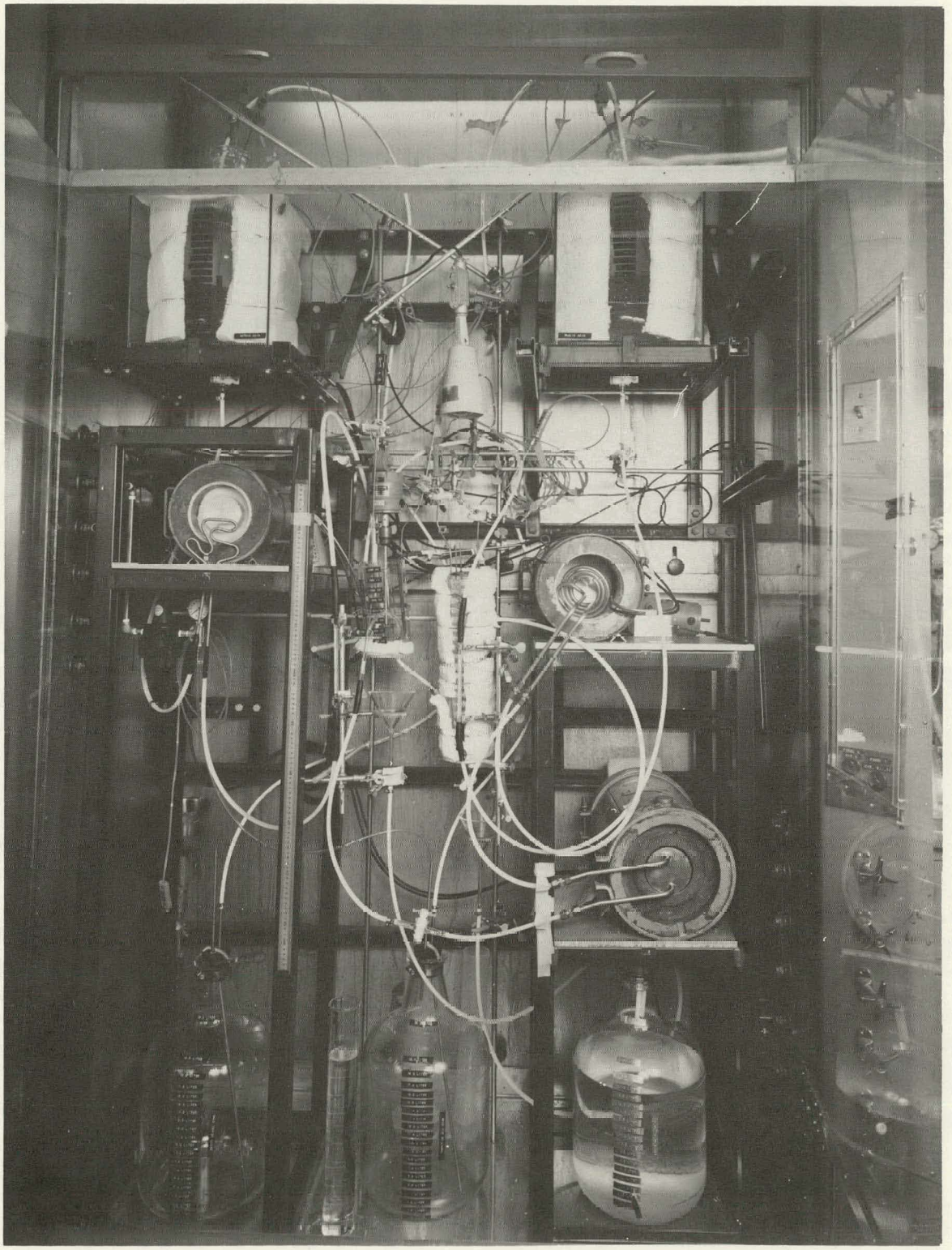

Fig. A.2. Actual equipment setup for single-STR experiments with continuous oxalate precipitation.

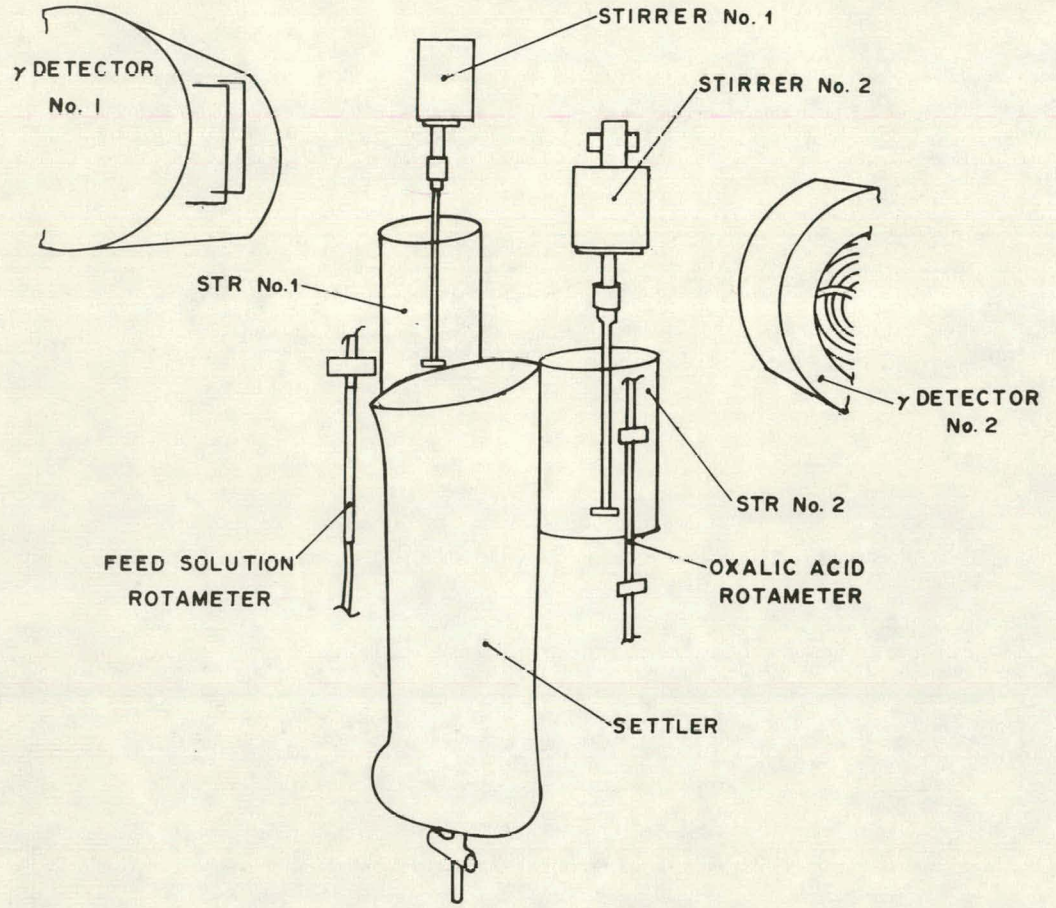

Fig. A.3. Components of experimental apparatus for continuous precipitation studies using two STRs in series.

ORNL-PHOTO 4519-77

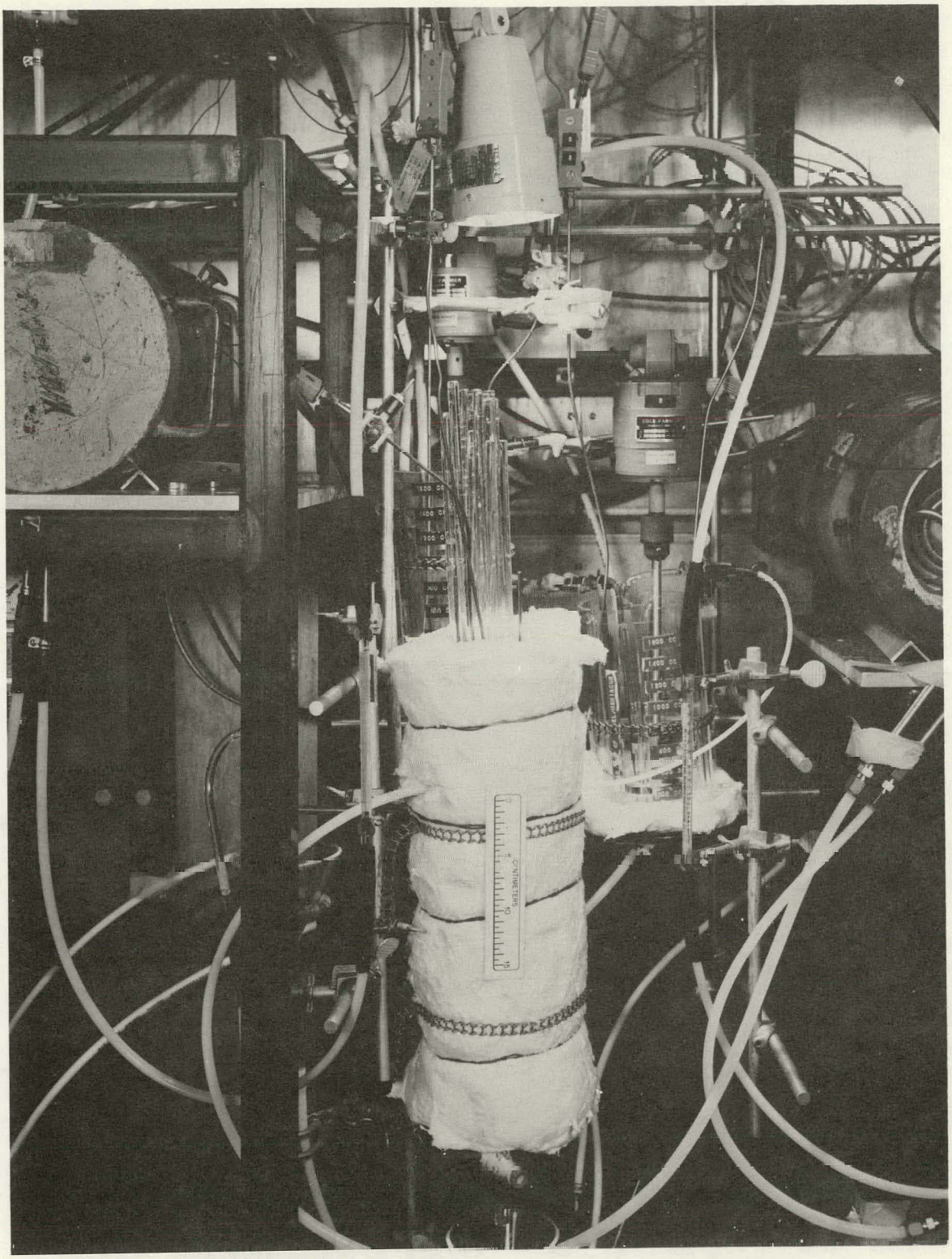

Fig. A.4. Actual equipment setup for experiments using two STRs in series.

ORNL-PHOTO 3483-77

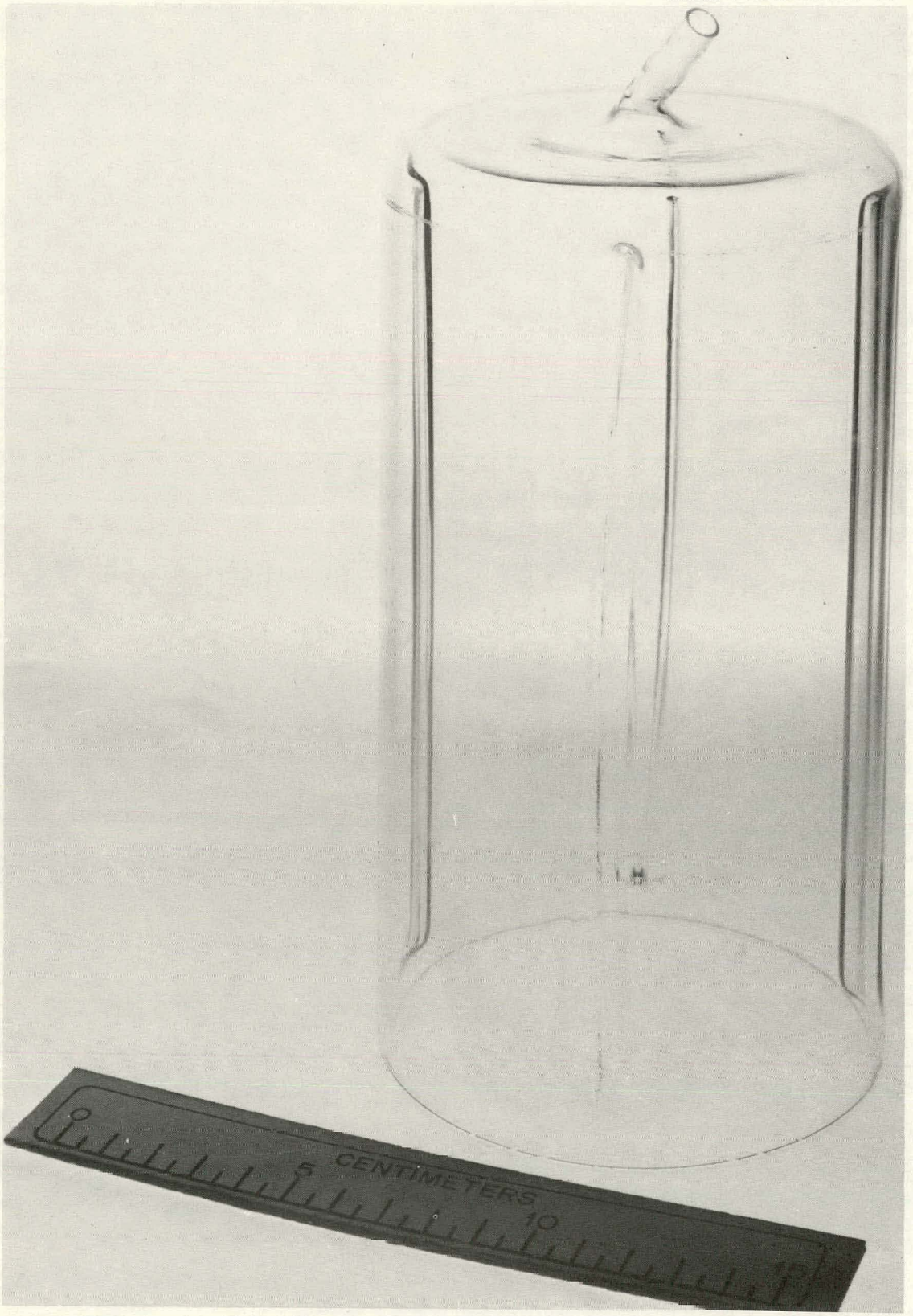

Fig. A.5. Stirred tank reactor.

ORNL-PHOTO 3484-77

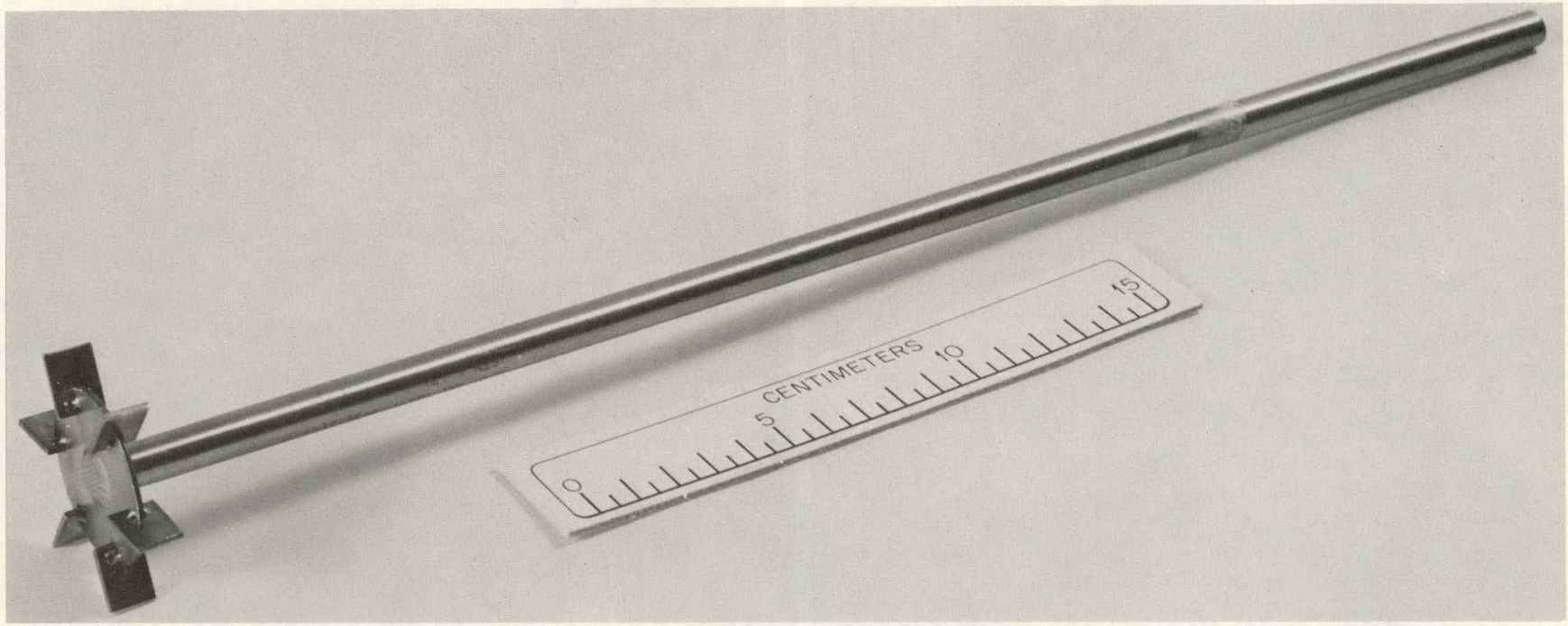

Fig. A.6. Impeller.

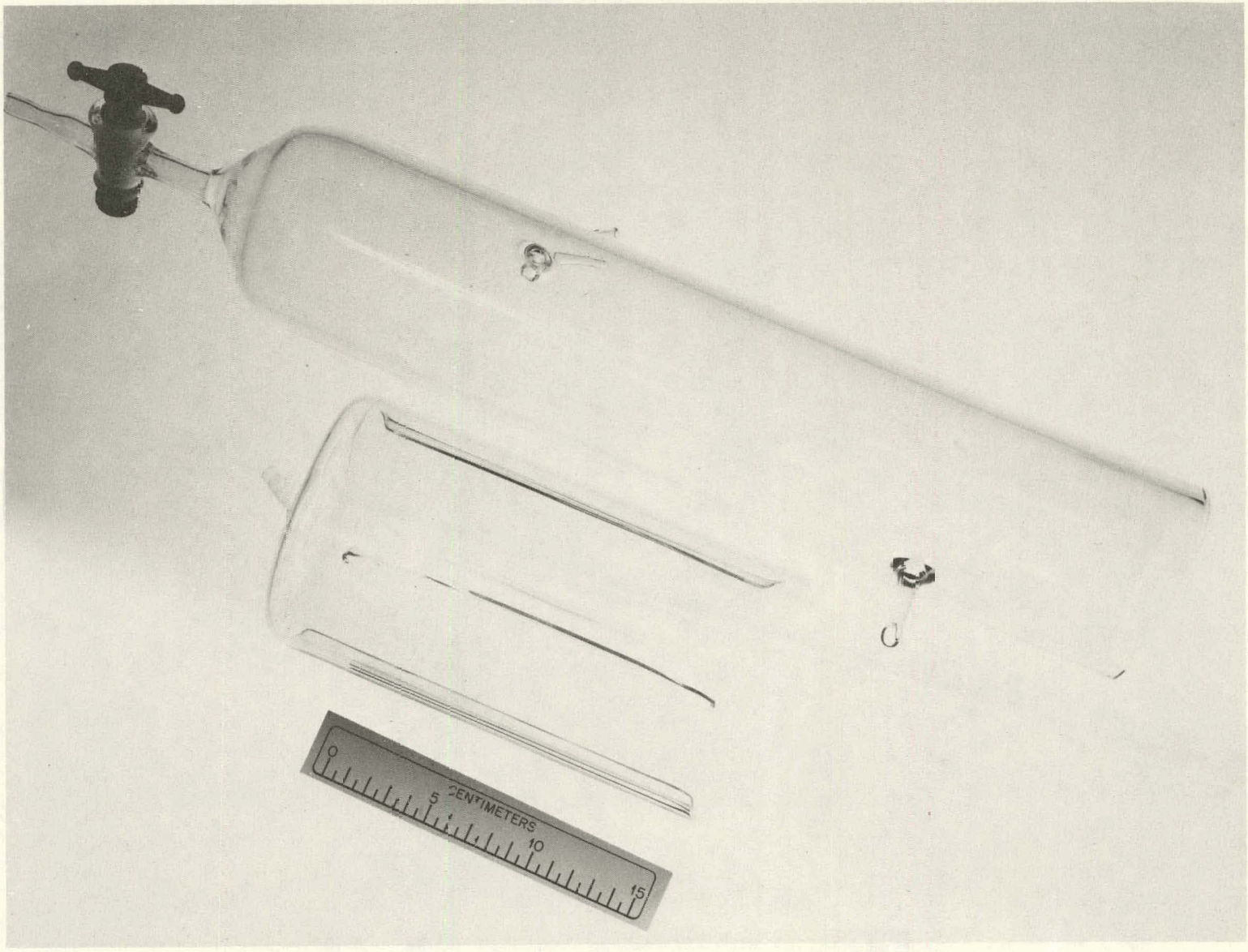

Fig. A.7. Settler and stirred tank reactor.

Appendix B. DATA FROM CHEMICAL ANALYSIS

THIS PAGE

WAS INTENTIONALLY

LEFT BLANK

Appendix B. DATA FROM CHEMICAL ANALYSIS

In many experiments, detailed chemical analysis of the precipitate and various liquid streams was conducted. These results were not reported in the body of the report due to uncertainty about the accuracy of certain analytical and calculative procedures. Instead, only the average composition of the precipitate was reported. This appendix provides detailed information on the chemical analysis, including the raw data.

B.1 Other Experiments

In addition to the run numbers prefixed by A and B (see Tables 3 and 4), a considerable number of runs were made in series labelled 0 and C. Chemical analysis of solids and liquids from these experiments were completed; hence, the experiments are described. Series C experiments, described in Appendix D, involved an alternative type of process system that seemed conceptually sound but proved to be experimentally problematic. Series 0 experiments were designed to check out experimental procedures, equipment, and analyses for the single-STR apparatus before carrying out the Series A experiments. Because the purpose of Series 0 experiments was to debug procedures and equipment, no radioactive tracers were used; therefore, the fraction of rare earths removed was not measured. The Series 0 experiments used only the settler for solid-liquid separation but had the same factorial experimental design as the Series A experiments. The solids and liquids generated by the Series 0 experiments were analyzed chemically. Table B.1 summarizes the operating conditions for this series.

B.2 Chemical Analysis

Various solid and liquid samples from the experiments were chemically analyzed by spark source mass spectrometry (Sect. 3.5). Table B.2 lists the sources of the samples used, and Tables B.3 through B.9 report the chemical analysis of these samples. Tables B.3 through B.9 provide two types of data: the raw mass spectrometer data and the calculated results.

Table B.1. Operating conditions for Series 0 experiments[a]

Run No.	Liquid residence time per reactor (min)	Reactor temperature (°C)	Oxalic acid concentration in stripper (M)	Mixing power[b] (W/liter)
5	22.3	27.25	0.212	1.74×10^{-1} (254 rpm)
6	10.1	26.85	0.197	3.23×10^{-2} (145 rpm)
7	22.3	54.70	0.212	1.70×10^{-2} (117 rpm)
8	10.1	53.50	0.197	1.72×10^{-1} (253 rpm)
9	22.4	27.25	0.308	3.95×10^{-2} (155 rpm)
10	9.8	27.25	0.289	1.81×10^{-1} (257.5 rpm)
11	9.8	52.05	0.289	2.12×10^{-2} (126 rpm)
12	22.4	51.10	0.308	1.36×10^{-1} (234 rpm)

[a]Conditions were nearly identical to Series A experiments; equipment was identical.

[b]Power $= \frac{(N_{Pr})\rho N^3 D^5}{g_c}$, where N_{Pr} (15) $= 5$; ρ = density = 1 g/cm^3; N = rev/min; D = impeller diam = 2.125 in.; $g_c = 3217$ lb·ft/lbf·sec^2.

Table B.2. Sources of samples listed in Tables B.3 through B.9

Table	Sample source
B.3	Precipitate from bottom of settler, liquid in contact with precipitate during entire experimental run, Series 0 experiments
B.4	Liquid from exit line of settler, Series 0 experiments
B.5	Precipitate from bottom of settler, Series A experiments
B.6	Liquid from exit line of settler, Series A experiments
B.7	Liquid from STR No. 1 after filtration by 12-, 5-, and 1-μm filters, Series A experiments
B.8	Series B precipitate after filtration by 12-, 5-, and 1-μm filters; Series C precipitate from bottom of settler
B.9	Series B liquid after filtration by 12-, 5-, and 1-μm filters; Series C liquid from exit line (see Appendix C)

Table B.3. Chemical analysis of solid precipitate, Series 0 experiments[a]

Element	Spark source mass spectrometer data										
			Sample No.								
	Feed[b]	Standard[b]	5A	5B	6	7	8	9	10	11	12
Praseodymium	100.00	100.00	100.00	100.00	100.00	100.00	100.00	100.00	100.00	100.00	100.00
Europium	14.25	32.00	28.35	30.96	33.75	31.68	36.21	29.25	36.57	37.57	33.12
Neodymium	341.97	540.00	630.00	602.00	630.00	624.00	639.00	540.00	689.00	600.00	540.00
Barium	138.86	220.00	0.72	0.65	1.08	100.80	1.21	1.58	2.12	1.15	1.01
Cesium	202.08	400.00	0.41	0.30	0.68	1.01	0.78	0.68	1.33	1.20	1.62
Molybdenum	284.98	120.00	0.08	0.11	0.18	0.09	0.18	0.23	0.19	0.17	0.13
Zirconium	303.11	100.00	4.50	4.30	4.50	4.80	7.10	4.50	5.30	5.00	3.60
Strontium	68.14	50.00	0.45	0.34	0.59	0.43	0.53	0.90	1.06	0.50	0.36
	Calculated percentage yields										
Praseodymium			100.00	100.00	100.00	100.00	100.00	100.00	100.00	100.00	100.00
Europium			88.59	96.75	105.47	99.00	113.16	91.41	114.28	117.19	103.50
Neodymium			116.67	111.48	116.67	115.56	118.33	100.00	127.59	111.11	100.00
Barium			0.33	0.30	0.49	45.82	0.55	0.72	0.96	0.52	0.46
Cesium			0.10	0.08	0.17	0.25	0.20	0.17	0.33	0.30	0.41
Molybdenum			0.07	0.09	0.15	0.08	0.15	0.19	0.16	0.14	0.11
Zirconium			4.50	4.30	4.50	4.80	7.10	4.50	5.30	5.00	3.60
Strontium			0.90	0.68	1.18	0.86	1.06	1.80	2.12	1.00	0.72

[a] All values are relative to praseodymium. It was assumed that all of the praseodymium precipitated.

[b] Standard used to calculate percentage yields. Standard is the feed solution for experiments listed. Feed spark source mass spectrometer data is the average analysis of the feed solution based on samples submitted at different times. It became evident that there was instrument drift with time; hence percent yields shown in each table are based on the analysis of the particular feed solution (labeled standard) which was analyzed simultaneously with samples 5A through 12.

Table B.4. Chemical analysis of liquids from settler exit, Series 0 experiments[a]

Sample	Spark source mass spectrometer data										
	Sample No.										
	Feed	Standard	5A	5B	6	7	8	9	10	11	12
Cesium	100.00	100.00	100.00	100.00	100.00	100.00	100.00	100.00	100.00	100.00	100.00
Europium	7.05	5.01	0.68	2.18	1.00	0.65	1.06	0.52	0.20	0.76	0.33
Neodymium	169.24	50.12	6.78	10.00	3.23	1.16	15.00	8.09	4.08	4.40	3.95
Praseodymium	49.49	8.41	0.78	1.27	0.81	0.38	2.25	1.76	0.84	1.04	0.90
Barium	68.72	57.28	31.33	50.00	29.72	18.63	16.25	47.60	19.18	36.00	39.51
Molybdenum	141.03	21.48	45.22	76.36	35.53	23.22	17.50	76.16	24.48	60.00	133.28
Zirconium	150.01	17.90	32.30	90.90	32.30	27.00	12.50	47.60	20.40	40.00	47.60
Strontium	33.72	10.74	9.37	16.36	9.69	6.48	4.13	13.80	4.69	11.60	11.90
	Calculated percentage yields										
Cesium			100.00	100.00	100.00	100.00	100.00	100.00	100.00	100.00	100.00
Europium			13.57	43.51	19.96	12.97	21.16	10.38	39.92	15.17	6.59
Neodymium			13.53	19.95	6.45	2.31	29.93	16.14	8.14	8.78	7.88
Praseodymium			9.28	15.10	9.63	4.52	26.75	20.93	9.99	12.37	10.70
Barium			54.70	87.29	51.89	32.52	28.37	83.10	33.49	62.85	68.98
Molybdenum			210.52	355.49	165.41	108.10	81.47	354.56	113.97	279.33	620.48
Zirconium			180.45	507.82	180.45	150.84	69.83	265.92	113.97	223.46	265.92
Strontium			87.24	152.33	90.22	60.34	38.45	128.49	43.67	108.01	110.80

[a]All values are relative to cesium. It was assumed that no cesium was carried in the oxalate precipitate.

Table B.5. Chemical analysis of precipitate from settler, Series A experiments[a]

Element	Spark source mass spectrometer data											
	Sample No.											
	Feed	Standard J	15J	16J	17J	18J	19J	20J	21J	22J	23J	24J
Praseodymium	100.00	100.00	100.00	100.00	100.00	100.00	100.00	100.00	100.00	100.00	100.00	100.00
Europium	14.25	43.85	49.28	41.50	54.67	55.00	35.28	47.25	55.61	41.58	50.05	31.50
Neodymium	341.97	613.90	708.40	647.40	770.00	720.00	616.00	661.50	747.00	63.00	693.00	63.00
Barium	138.86	263.10	2.46	1.16	1.23	0.70	1.46	2.70	1.74	0.97	1.31	0.59
Cesium	202.08		1.14	1.25	1.31	0.50	0.90	1.35	0.75	1.93	1.54	0.90
Ruthenium	178.24	315.72	0.63	0.48	0.41	0.19	0.47	0.58	0.25	0.42	0.50	0.18
Molybdenum	284.98	192.94	0.71	0.49	0.41	0.20	0.44	0.72	0.29	0.42	0.46	0.18
Zirconium	303.11	175.40	15.40	8.30	7.70	10.00	5.60	13.50	8.30	4.20	7.70	4.50
Strontium	68.14	64.90	1.11	0.83	0.50	0.43	0.78	1.76	0.83	0.34	0.77	0.32
	Calculated percentage yields											
Praseodymium			100.00	100.00	100.00	100.00	100.00	100.00	100.00	100.00	100.00	100.00
Europium			112.38	94.64	124.68	125.43	80.46	107.75	126.82	94.82	114.14	71.84
Neodymium			115.39	105.46	125.43	117.28	100.34	107.75	121.68	10.26	112.89	10.26
Barium			0.94	0.44	0.47	0.27	0.56	1.03	0.66	0.37	0.50	0.22
Cesium												
Ruthenium			0.20	0.15	0.13	0.06	0.15	0.18	0.08	0.13	0.16	0.06
Molybdenum			0.37	0.25	0.21	0.10	0.23	0.37	0.15	0.22	0.24	0.09
Zirconium			8.78	4.73	4.39	5.70	3.19	7.70	4.73	2.40	4.39	2.57
Strontium			1.71	1.28	0.77	0.66	1.20	2.71	1.28	0.52	1.19	0.49

[a]All values are relative to praseodymium.

Table B.6. Chemical analysis of liquids from settler, Series A experiments[a]

Element	Spark source mass spectrometer data											
	Sample No.											
	Feed	Standard K	15K	16K	17K	18K	19K	20K	21K	22K	23K	24K
Cesium	145.53											
Europium	10.26	16.67	2.53	14.46	0.84	1.67	0.71	0.91	1.33		1.51	0.54
Neodymium	246.27	241.67	20.58	16.87	17.39	15.15	7.85	5.91	14.46		7.42	4.69
Praseodymium	72.02	39.17	4.94	12.05	21.74	3.79	1.67	1.27	3.25	1.30	1.51	1.15
Barium	100.00	100.00	100.00	100.00	100.00	100.00	100.00	100.00	100.00	100.00	100.00	100.00
Ruthenium	128.36	125.00	158.76	204.85	152.18	242.40	204.68	181.80	132.55	217.40	150.50	130.73
Molybdenum	205.23	83.33	106.43	116.89	100.00	151.50	130.90	118.17	86.76	130.44	99.98	84.59
Zirconium	218.29	83.33	58.80	120.50	108.70	151.50	119.00	90.90	120.50	108.70	107.50	76.90
Strontium	49.07	28.33	31.75	36.15	29.35	34.85	26.18	26.36	28.92	28.26	30.10	27.68
	Calculated percentage yields											
Cesium												
Europium			15.18	86.74	5.04	10.02	4.26	5.46	7.98		9.06	3.24
Neodymium			8.52	6.98	7.20	6.27	3.25	2.45	5.98		3.07	1.94
Praseodymium			12.61	30.76	55.50	9.68	4.26	3.24	8.30	3.32	3.86	2.94
Barium			100.00	100.00	100.00	100.00	100.00	100.00	100.00	100.00	100.00	100.00
Ruthenium			127.01	163.88	121.74	193.92	163.74	145.44	106.04	173.92	120.40	104.58
Molybdenum			127.72	140.27	120.01	181.81	157.09	141.81	104.12	156.53	119.98	101.51
Zirconium			70.56	144.61	130.45	181.81	142.81	109.08	144.61	130.45	129.01	92.28
Strontium			112.07	127.60	103.60	123.01	92.41	93.05	102.08	99.75	106.25	97.71

[a]All values are relative to barium.

Table B.7. Chemical analysis of liquids after filtration, Series A experiments[a]

Element	Spark source mass spectrometer data											
	Sample No.											
	Feed	Standard L	15L	16L	17L	18L	19L	20L	21L	22L	23L	24L
Cesium	145.53											
Europium	10.26	16.67	2.58		3.00	7.73						1.45
Neodymium	246.27	211.11	10.31	13.13	21.00	139.38	13.33		6.42	4.25	7.79	29.03
Praseodymium	72.02	34.44	2.58	1.92	3.60	27.27	2.28	1.77	1.73	0.82	1.54	5.81
Barium	100.00	100.00	100.00	100.00	100.00	100.00	100.00	100.00	100.00	100.00	100.00	100.00
Ruthenium	128.36	83.33	154.65	141.40	150.00	287.85	228.02	189.90	197.60	205.50	144.30	306.47
Molybdenum	205.23	55.56	103.10	89.89	90.00	181.80	147.34	120.27	135.85	132.89	96.20	193.56
Zirconium	218.29	55.56	103.10	101.00	100.00	151.50	175.40	126.60	123.50	137.00	96.20	161.30
Strontium	49.07	21.11	32.99	31.31	30.00	31.82	38.59	36.71	29.64	28.77	32.71	33.87
	Calculated percentage yields											
Cesium												
Europium			15.48		13.00	46.37						8.70
Neodymium			4.88	6.22	9.95	66.02	6.31		3.04	2.01	3.69	13.75
Praseodymium			7.49	5.58	10.45	79.18	6.62	5.14	5.02	2.38	4.47	16.87
Barium			100.00	100.00	100.00	100.00	100.00	100.00	100.00	100.00	100.00	100.00
Ruthenium			135.59	169.69	180.01	345.43	273.64	227.89	237.13	246.61	173.17	367.78
Molybdenum			135.57	161.79	161.99	327.21	265.19	216.47	244.51	239.18	173.15	348.38
Zirconium			135.57	181.79	179.99	272.68	315.70	227.86	222.28	246.58	173.15	290.32
Strontium			156.28	148.32	142.11	150.73	182.80	173.90	140.41	136.29	154.95	160.45

[a]All values are relative to barium.

Table B.8. Chemical analysis of solid precipitates, Series B and Series C experiments[a]

Element	Spark source mass spectrometer data, Sample No.				Calculated percentage yields, Sample No.			
	27S[b]	34S[b]	41P[b]	45P[b]	27S[b]	34S[b]	41P[b]	45P[b]
Praseodymium	100.000	100.000	100.000	100.000	100.000	100.000	100.000	100.000
Holmium	≤0.073	≤0.036	≤0.167	≤0.046	912.500	450.000	2087.500	575.000
Dysprosium	0.545	0.336	0.833	0.345	524.038	323.077	800.962	331.731
Terbium	3.455	1.545	5.833	1.092	(3.455)	(1.545)	(5.833)	(1.092)
Gadolinium	36.364	31.818	86.667	26.437	369.365	323.189	880.315	268.532
Europium	56.364	39.091	71.667	57.471	128.538	89.147	163.437	131.063
Samarium	218.182	163.636	316.667	241.379	294.470	220.852	427.391	325.778
Neodymium	727.273	636.364	950.000	747.126	118.468	103.659	154.748	121.702
Cerium	181.818	136.364	138.333	159.770	88.168	66.126	67.081	77.476
Lanthanum	83.636	90.909	64.167	57.471	78.740	85.587	60.411	54.107
Barium	2.364	0.864	1.167	0.402	0.899	0.328	0.444	0.153
Cesium	1.273	1.000	0.833	0.184	0.630	0.495	0.412	0.091
Tellurium	1.036	0.545	0.500	0.195	2.209	1.162	1.066	0.416
Antimony	0.109	≤0.027			10.521	2.606		
Tin	1.018	0.455	0.833	0.161	24.560	10.977	20.097	3.884
Indium	≤0.055	≤0.018			52.885	17.308		
Cadmium	0.145	≤0.055			2.073	0.786		
Palladium	1.455	0.909	1.667	0.414	1.232	0.769	1.411	0.350
Rhodium	0.164	0.091	0.133	0.057	0.506	0.281	0.411	0.176
Ruthenium	0.400	0.364	≤0.017		0.127	0.115	0.005	
Molybdenum	0.636	0.391	0.333	0.115	0.330	0.203	0.173	0.060
Niobium								
Zirconium	18.182	9.091	16.667	11.494	10.366	5.183	9.502	6.553
Yttrium	26.364	18.182	16.667	19.540	67.245	46.376	42.511	49.839
Strontium	1.091	0.473	0.733	0.402	1.681	0.729	1.129	0.619
Rubidium	0.236	0.173	0.150	0.046	0.851	0.624	0.541	0.166
Selenium								
Iron		0.036	0.117	0.069		(0.036)	(0.177)	(0.069)

[a] All numbers are relative to praseodymium.

[b] Samples 27S and 34S are from Series B experiments; samples 41P and 45P are from Series C experiments.

Table B.9. Chemical analysis of liquids after filtration, Series B and Series C experiments[a]

Element	Spark source mass spectrometer data, Sample No.						Calculated percentage yields, Sample No.					
	27P[b]	27Q[b]	34P[b]	34Q[b]	41S[b]	45S[b]	27P[b]	27Q[b]	34P[b]	34Q[b]	41S[b]	45S[b]
Barium	100.000	100.000	100.000	100.000	100.000	100.000	100.000	100.000	100.000	100.000	100.000	100.000
Gadolinium	≤8.722						123.018					
Europium		2.333	4.167	≤1.493	≤2.500	≤3.704		13.995	24.997	8.956	14.997	22.220
Samarium												
Neodymium	≤10.526	12.500	10.417	≤7.463	≤12.500	≤14.815	4.356	5.172	4.310	3.088	5.172	6.130
Praseodymium	2.632	2.833	2.083	1.493	2.500	2.963	6.719	7.233	5.318	3.812	6.382	7.564
Cerium	8.421	9.333	5.208	5.075	7.500	10.000	5.670	6.285	3.507	3.417	5.050	6.734
Lanthanum	8.772	10.333	6.250	5.224	8.250	12.222	11.468	13.508	8.171	6.829	10.785	15.978
Cesium	210.526	216.667	375.000	149.254	250.000	277.778	144.670	148.890	257.695	102.565	171.795	190.884
Tellurium	126.316	150.000	187.500	111.940	217.500	107.407	374.059	444.194	555.243	331.487	644.082	318.064
Antimony					≤2.500						335.121	
Tin		5.000		≤2.985	17.500			167.504		100.000	586.265	
Indium		0.500						666.667				
Cadmium	15.789	16.667	25.000	14.925	20.000		313.460	330.891	496.327	296.307	397.062	
Palladium	350.877	325.000	447.917	253.731	550.000	296.296	412.433	382.016	526.497	298.244	646.488	348.276
Rhodium	114.035	108.333	137.500	74.627	162.500	111.111	488.980	464.530	589.597	319.999	696.797	476.442
Ruthenium	210.526	195.000	229.167	123.881	≤2.500	≤7.407	168.421	156.000	183.334	99.105	2.000	5.926
Molybdenum	140.351	121.667	125.000	79.104	172.500	103.704	168.428	146.006	150.006	94.929	207.008	124.450
Zirconium	140.351	125.000	141.667	86.567	130.000	125.926	168.428	150.006	170.007	103.885	156.006	151.117
Yttrium	1.754	2.333		1.045	2.000	2.593	6.212	8.263		3.701	7.084	9.184
Strontium	36.842	33.333	37.500	26.866	35.000	33.333	130.046	117.660	132.369	94.832	123.544	117.660
Rubidium	64.912	75.000	89.583	43.284	100.000	66.667	325.162	375.695	448.745	216.821	500.927	333.953
Selenium		4.667	6.250	2.836	9.250	≤3.333		156.348	209.380	95.008	309.883	111.658
Zinc	0.526	1.000	2.083	0.746	3.500		(0.526)	(1.000)	(2.083)	(0.746)	(3.500)	
Copper		0.667	1.667		1.750			(0.667)	(1.667)		(1.750)	
Nickel					1.250						(1.250)	
Iron	4.737	1.833	2.500	1.940	6.750	6.667	(4.737)	(1.833)	(2.500)	(1.940)	(6.750)	(6.667)
Manganese		0.667						(0.667)				
Calcium	4.737	3.833					(4.737)	(3.833)				
Potassium	1.053	1.333					(1.053)	(1.333)				
Sulfur	10.877	10.000					(10.877)	(10.000)				
Phosphorus	0.175						(0.175)					
Silicon	8.772	10.000					(8.772)	(10.000)				
Aluminum	1.228	1.667					(1.228)	(1.667)				
Magnesium	3.509	13.333					(3.509)	(13.333)				
Sodium	17.544	33.333					(17.544)	(33.333)				
Boron	0.702						(0.702)					

[a] All numbers are relative to barium.

[b] Samples 27P, 27Q, 34P, and 34Q are from Series B experiments; samples 41S and 45S are from Series C experiments.

A factorial analysis was made on the europium percentage yield of the precipitate for Series B experiments as a function of system temperature, oxalic acid concentration, liquid slurry residence time in the reactor, and impeller stirrer speed. The percentage yield, which varies from 88.59 to 117.19% in Table B.3, measures the fraction of europium precipitated compared to the fraction of praseodymium precipitated. The factorial error analysis indicates that the uncertainty in analysis was significantly larger than any variation in yield due to variations in operating conditions. In effect, all results were buried in the uncertainty of the chemical analyses.

Several other statistical analyses yielded similar results; hence, it was concluded that further statistical analyses, except those used to determine average composition of the precipitate and its standard deviation, were unwarranted. The raw data are included here so that other types of analyses may be made if the reader wishes to do so.

THIS PAGE

WAS INTENTIONALLY

LEFT BLANK

Appendix C. LEAST SQUARES FIT OF DATA

THIS PAGE

WAS INTENTIONALLY

LEFT BLANK

Appendix C. LEAST SQUARES FIT OF DATA

The factorial analysis used in these experiments assumes that the product yield is a linear function of the independent variables. This assumption greatly aids interpretation of data and is a reasonable assumption for small changes in any single variable. A question exists, however, as to whether or not some characteristics of the system have been hidden by the analysis. By use of a least squares analysis, the data can be examined from a different viewpoint, and additional insight can be obtained. This additional analysis was only done for the Series B experiments (i.e., those experimental runs which used two STRs in series). The details of this analysis are shown here.

C.1 Least Squares Analysis Used on Data

The data was analyzed by the SAS.76 computer program (see ref. 21, Sect. 6). This program, which uses a least squares technique, finds the best linear equation to fit the raw data. For example, if there are three variables as a function of Y, the program fits the data to all of the linear equations that are possible with three variables, as shown in Table C.1. The program then determines which equation best fits the data.

For the analysis herein, all of the variables listed in the first column of Table C.2 were considered as independent variables. The variables included all independent experimental variables and the cross products of these variables. The time variable ET is in the exponential form to allow time to enter as an exponential in a linear equation. This was included because product yield is expected to vary with time in the form $1 - e^{-t}$. The coefficient of correlation, R^2, was calculated for each equation and was used to infer the best fit of the data (Sect. 4.3). Given a fixed number of data sets, the equation which gives an R^2 value that is nearest to unity is said to be the best fit.

Table C.3 lists the most important variables to maximize product yield from STR No. 1 of the experiments that used two STRs (Series B experiments). For one-, two-, three-, and four-variable linear equations,

Table C.1. Equations used to fit data for three variables

One-variable equations
$Y = A_0 + A_1X_1$
$Y = A_0 + A_2X_2$
$Y = A_0 + A_3X_3$
Two-variable equations
$Y = A_0 + A_1X_1 + A_2X_2$
$Y = A_0 + A_1X_1 + A_3X_3$
$Y = A_0 + A_2X_2 + A_3X_3$
Three-variable equation
$Y = A_0 + A_1X_1 + A_2X_2 + A_3X_3$

Table C.2. Variables for least squares analysis

Variable abbreviation	Variable name	Units
W1	Power to STR No. 1	W/liter
T	Time	min
TMP	Temperature	°C
COOH	Oxalic acid concentration	mole/liter
W2	Power to STR No. 2	W/liter
ET	Exponential time, $10^{13} \times e^{-t}$	None
WW	Power to STR No. 1 x power to STR No. 2	$(W/liter)^2$
W1T	Power to STR No. 1 x time	W·min/liter
W2T	Power to STR No. 2 x time	W·min/liter
TTMP	Time x temperature	min·°C
CT	Oxalic acid concentration x time	mole·min/liter
CTMP	Oxalic acid concentration x temperature	mole·°C/liter
CW1	Oxalic acid concentration x power to STR No. 1	$mole \cdot W/liter^2$
CW2	Oxalic acid concentration x power to STR No. 2	$mole \cdot W/liter^2$
W1TMP	Power to STR No. 1 x temperature	W·°C/liter
W2TMP	Power to STR No. 2 x temperature	W·°C/liter
W12	Power to STR No. 1, squared	$(W/liter)^2$
W22	Power to STR No. 2, squared	$(W/liter)^2$
COOH2	Oxalic acid concentration, squared	$(mole/liter)^2$
T2	Time, squared	min^2
TMP2	Temperature, squared	$°C^2$

Table C.3. Best least squares equations for STR No. 1, Series B experiments

Number of variables in equation	Solid-liquid separation with 12-μm filter					Solid-liquid separation with 12-μm filter				
	Best variables				R^2	Best variables				R^2
1	CT				0.5941	TMP2				0.2570
1	TMP2				0.5598	TMP				0.2564
1	TMP				0.5580	COOH				0.2519
1	ET				0.4889	CT				0.2516
1	COOH				0.4024	W12				0.2503
1	CTMP				0.3902	CTMP				0.2479
2	ET	CTMP			0.8565	W1T	W12			0.6761
2	ET	COOH2			0.8563	W1T	W1TMP			0.6110
2	COOH	ET			0.8542	W1	W1T			0.5957
2	TMP	TMP2			0.7700	W12	CT			0.4848
2	T	COOH			0.7685	W1	W1TMP			0.4770
2	COOH	T			0.7677	W1TMP	CT			0.4671
3	TMP	W1T	TMP2		0.8890	W1T	W12	CTMP		0.8720
3	W1T	ET	CTMP		0.8829	W1T	W12	COOH2		0.8713
3	COOH	W1T	ET		0.8809	COOH	W1T	W12		0.8684
3	W1T	ET	COOH2		0.8797	COOH	W1T	W1TMP		0.8555
3	TMP	TT	TMP2		0.8754	W1T	W1TMP	CTMP		0.8549
3	T	TMP	TMP2		0.8749	COOH	W1	W1T		0.8527
4	TMP	W1T	CW1	TMP2	0.9866	COOH	W1T	W12	ET	0.9614
4	W1	TMP	W1T	TMP2	0.9753	W1T	W12	ET	CTMP	0.9615
4	TMP	W1T	W1TMP	TMP2	0.9745	W1T	W12	ET	COOH2	0.9603
4	TMP	W1T	W12	TMP2	0.9690	W1T	W12	CT	COOH2	0.9433
4	TT	CT	CTMP	T2	0.9645	COOH	W1T	W1TMP	T2	0.9403
4	TT	CT	COOH2	T2	0.9633	W1T	W12	CT	CTMP	0.9378

the best six equations of each form are given. For example, the best equation using two variables as a linear equation of product yield from STR No. 1 with solid-liquid separation by 12-μm filter in Series B experiments is $Y = A_0 + (A_1 \times ET) + (A_2 \times CTMP)$ with an R^2 value of 0.8565. The next best equation, $Y = A_0 + (A_1 \times ET) + (A_2 \times COOH2)$, has an R^2 value of 0.8563.

Several observations about this approach are noteworthy. First, equations with larger numbers of variables have higher R^2 values, as would be expected. Second, in many cases different equations can represent the data almost equally well. In most cases, however, equations with equally good fit have the same basic variables but the form of the variables is rearranged.

After determination of the best equations with which to fit the data, the coefficients of those equations were determined. The results for Series B experiments are shown in Tables C.6 through C.10; definitions of the variables are given in Tables C.4 and C.5. For each set of data, the coefficients for the best two equations for one, two, three, and four variables were determined. All of the equations are written in three forms, as discussed below.

The first equation form fit the raw data as obtained. For example, consider the first one-variable equation of product yield for STR No. 1, Series B experiments, with solid-liquid separation by 12-μm filter as shown in Table C.7. Here R^2 equals 0.594, the intercept equals 36.379, and the coefficient of CT is 3.867. The resultant equation is

$$Y = 36.379 + (3.867 \times CT) , \qquad (C.1)$$

where Y is product yield (%), and CT is oxalic acid concentration (mole/liter) x residence time of liquid in each reactor (min).
The second alternative one-variable equation is

$$Y = 779.655 - (0.519 \times TMP^2) . \qquad (C.2)$$

Equations C.1 and C.2 are useful, but one cannot easily compare the importance of the variable CT compared to TMP^2 on product yield. To determine the relative importance of different variables, the equations must be written in some form that will put each variable on a common basis. Two such approaches were adopted.

Table C.4. Normalized variables for STR No. 1, Series B experiments[a]

Raw data variable	W1	T	TMP	COOH	ET
Variable definition	Power to STR No. 1	Time	Temperature	Oxalic acid concentration	Exponential time
Units	W/liter	min	°C	mole/liter	None
[-1, +1] normalized variable	$\overline{W1}$	$\overline{T}$	$\overline{TMP}$	$\overline{COOH}$	$\overline{ET}$
Variable definition	$\frac{W1 - 0.09}{0.09}$	$\frac{T - 30}{10}$	$\frac{TMP - 37}{5}$	$\frac{COOH - 0.25}{0.05}$	$\frac{ET - 1.06 \times 10^4}{1.0 \times 10^4}$
Sigma normalized variable	$\overline{\overline{W1}}$	$\overline{\overline{T}}$	$\overline{\overline{TMP}}$	$\overline{\overline{COOH}}$	$\overline{\overline{ET}}$
Variable definition	$\frac{W1 - 0.095}{0.077}$	$\frac{T - 29.664}{8.777}$	$\frac{TMP - 38.109}{0.236}$	$\frac{COOH - 0.244}{0.041}$	$\frac{ET - 8141.92}{11,317.235}$
Sigma normalized variable	$\overline{\overline{W1T}}$	$\overline{\overline{TT}}$	$\overline{\overline{CT}}$	$\overline{\overline{CTMP}}$	$\overline{\overline{CW1}}$
Variable definition	$\frac{W1T - 2.819}{2.602}$	$\frac{TT - 1100.34}{324.844}$	$\frac{CT - 7.212}{2.431}$	$\frac{CTMP - 9.031}{1.472}$	$\frac{CW1 - 0.023}{0.019}$
Sigma normalized variable	$\overline{\overline{W1TMP}}$	$\overline{\overline{TMP2}}$	$\overline{\overline{T2}}$	$\overline{\overline{COOH2}}$	$\overline{\overline{W12}}$
Variable definition	$\frac{W1TMP - 3.515}{2.873}$	$\frac{TMP2 - 1377.14}{17.562}$	$\frac{T2 - 949.955}{524.655}$	$\frac{COOH2 - 0.061}{0.063}$	$\frac{W12 - 0.014}{0.017}$

[a] Cross terms for raw data variables and [-1, +1] normalized variables are obtained by simply multiplying the appropriate variables together; for example, CTMP = COOH x TMP, and $\overline{CTMP} = \overline{COOH} \times \overline{TMP}$. For sigma normalized variables this procedure is invalid because the mean of COOH times the mean of TMP (or any other variable) is not the mean (except in special cases) of COOH x TMP.

Table C.5. Normalized variables for STR No. 2, Series B experiments[a]

Raw data variable	W1	T	TMP	COOH	W2	ET
Variable definition	Power to STR No. 1	Time	Temperature	Oxalic acid concentration	Power to STR No. 2	Exponential time
Units	W/liter	min	°C	mole/liter	W/liter	None
[-1, +1] normalized variable	$\overline{W1}$	$\overline{T}$	$\overline{TMP}$	$\overline{COOH}$	$\overline{W2}$	$\overline{ET}$
Variable definition	$\frac{W1 - 0.09}{0.09}$	$\frac{T - 30}{10}$	$\frac{TMP - 35}{5}$	$\frac{COOH - 0.25}{0.05}$	$\frac{W2 - 0.09}{0.09}$	$\frac{ET - 1.0 \times 10^4}{1.0 \times 10^4}$
Sigma normalized variable	$\overline{\overline{W1}}$	$\overline{\overline{T}}$	$\overline{\overline{TMP}}$	$\overline{\overline{COOH}}$	$\overline{\overline{W2}}$	$\overline{\overline{ET}}$
Variable definition	$\frac{W1 - 0.095}{0.007}$	$\frac{T - 29.664}{8.777}$	$\frac{TMP - 35.666}{0.544}$	$\frac{COOH - 0.244}{0.041}$	$\frac{W2 - 0.089}{0.068}$	$\frac{ET - 8141.92}{11,317.24}$
Sigma normalized variable	$\overline{\overline{WW}}$	$\overline{\overline{W1T}}$	$\overline{\overline{W2T}}$	$\overline{\overline{TT}}$	$\overline{\overline{CT}}$	$\overline{\overline{CTMP}}$
Variable definition	$\frac{WW - 0.009}{0.012}$	$\frac{W1T - 2.819}{2.603}$	$\frac{W2T - 2.623}{2.176}$	$\frac{TT - 1055.28}{304.26}$	$\frac{CT - 7.212}{2.431}$	$\frac{CTMP - 8.676}{1.394}$
Sigma normalized variable	$\overline{\overline{CW1}}$	$\overline{\overline{CW2}}$				
Variable definition	$\frac{CW1 - 0.023}{0.019}$	$\frac{CW2 - 0.022}{0.017}$				

[a] Cross terms for raw data variables and [-1, +1] normalized variables are obtained by simply multiplying the appropriate variables together; for example, CTMP = COOH x TMP, and $\overline{CTMP} = \overline{COOH} \times \overline{TMP}$. For sigma normalized variables this procedure is invalid because the mean of COOH times the mean of TMP, for example, is not the mean of COOH x TMP except in special cases.

Table C.6. Least squares equation coefficients of product yield (%) of STR No. 1, Series B experiments, with solid-liquid separation by 1-μm filter

	Raw data fit	[-1, +1] normalization	Sigma normalization		Raw data fit	[-1, +1] normalization	Sigma normalization
	One-variable models				Three-variable models		
R^2	0.257	0.316	0.267	R^2	0.872	0.876	0.872
Intercept	324.906	81.354	78.885	Intercept	61.148	82.694	78.585
TMP2	-0.179	-1103.723	-3.141	CTMP	1.871	74.751	2.754
				W1T	3.305	4.949	8.605
R^2	0.256	0.256	0.256	W12	-610.642	-2.993	-10.467
Intercept	570.918	80.632	78.585				
TMP	-13.267	-66.336	-3.137	R^2	0.871	0.721	0.871
				Intercept	69.648	83.319	78.885
				W1T	3.302	5.041	8.597
				W12	-612.731	-5.608	-10.502
				COOH2	138.753	-1.647	2.746
	Two-variable models				Four-variable models		
R^2	0.676	0.715	0.676	R^2	0.961	0.914	0.961
W1T	3.344	5.052	78.585	Intercept	57.862	82.092	78.585
W12	-630.699	-6.744	8.706	COOH	67.574	3.309	2.752
Intercept	78.227	83.062	-10.810	W1T	5.389	4.915	14.030
				W12	-920.637	-4.904	-15.780
R^2	0.611	0.616	0.611	ET	0.0002840	-0.875	3.214
Intercept	82.235	78.774	78.585				
W1T	3.238	4.269	8.430	R^2	0.961	0.883	0.961
W1TMP	-3.636	-55.108	-10.448	Intercept	57.518	82.324	78.585
				W1T	5.369	4.822	13.978
				W12	-917.777	-2.672	-15.731
				ET	0.0002731	-0.525	3.147
				CTMP	1.867	72.760	2.749

Table C.7. Least squares equations of product yield (%) of STR No. 1, Series B experiments, with solid-liquid separation by 12-μm filter

	Raw data fit	[-1, +1] normalization	Sigma normalization
	One-variable models		
R^2	0.594	0.183	0.594
Intercept	36.379	64.131	64.264
CT	3.867	-6.398	9.398
R^2	0.559	0.766	0.554
Intercept	779.655	72.757	64.264
TMP2	-0.519	-3385.093	-9.123
	Two-variable models		
R^2	0.857	0.815	0.857
Intercept	24.878	68.270	64.264
ET	-0.0007359	-5.596	-8.329
CTMP	5.025	175.438	7.395
R^2	0.855	0.570	0.856
Intercept	47.544	68.115	64.264
ET	-0.0007371	-6.391	-8.342
COOH2	373.575	-8.132	7.393

	Raw data fit	[-1, +1] normalization	Sigma normalization
	Three-variable models		
R^2	0.889	0.884	0.889
Intercept	-182326.467	72.652	64.264
TMP	9862.029	-34.533	2331.888
W1T	1.626	4.969	4.235
TMP2	-133.309	-3063.427	-2341.138
R^2	0.883	0.851	0.883
Intercept	21.336	68.410	64.264
W1T	0.783	2.815	2.040
ET	-0.0007	-5.223	-7.864
CTMP	5.135	178.891	7.558
	Four-variable models		
R^2	0.987	0.920	0.987
Intercept	-172363.289	72.905	64.264
TMP	9329.905	-47.415	2206.067
W1T	4.009	4.872	10.438
CW1	-388.428	-3.030	-7.363
TMP2	-126.203	-3102.254	-2216.348
R^2	0.975	0.918	0.975
Intercept	-157,574.2	72.935	64.264
W1	-105.408	2.671	-8.138
TMP	8527.088	-25.138	2016.240
W1T	4.369	5.033	11.374
TMP2	-115.309	-3313.433	-2025.028

Table C.8. Least squares model for STR No. 2, Series B experiments

Number of variables in equation	Solid-liquid separation with 12-μm filter					Solid-liquid separation with 12-μm filter				
	Best variables				R^2	Best variables				R^2
1	CT				0.5614	CT				0.5080
1	TMP2				0.5434	TMP2				0.4906
1	TMP				0.5391	TMP				0.4874
1	ET				0.5219	ET				0.4546
1	T				0.3523	T				0.3081
1	TTMP				0.3314	TTMP				0.2878
2	ET	CTMP			0.7522	ET	CW2			0.7461
2	COOH	ET			0.7593	CT	CW2			0.6824
2	ET	COOH2			0.7590	CT	W2TMP			0.6672
2	TMP	TMP2			0.7037	W2	CT			0.6638
2	ET	CW2			0.6974	ET	W2TMP			0.6580
2	T	COOH			0.6455	ET	CTMP			0.6563
3	ET	CTMP	W2TMP		0.8954	W2T	ET	CW2		0.8951
3	ET	CTMP	W22		0.8926	ET	CTMP	W2TMP		0.8876
3	W2	ET	CTMP		0.8912	W2	ET	CTMP		0.8818
3	COOH	ET	W2TMP		0.8834	ET	CTMP	W22		0.8787
3	ET	W2TMP	COOH2		0.8808	COOH	ET	W2TMP		0.8758
3	COOH	ET	W22		0.8805	ET	CTMP	CW2		0.8742
4	W2	ET	W2TMP	COOH2	0.9761	W2	ET	CTMP	W2TMP	0.9763
4	W2	ET	CTMP	W2TMP	0.9760	W2	ET	W2TMP	COOH2	0.9752
4	COOH	W2	ET	W2TMP	0.9745	COOH	W2	ET	W2TMP	0.9747
4	W2T	ET	CTMP	W22	0.9682	W2T	ET	CTMP	W22	0.9719
4	COOH	W2T	ET	W22	0.9649	W2T	ET	CTMP	W2TMP	0.9709
4	W2T	ET	COOH2	W22	0.9633	W2T	ET	W2TMP	COOH2	0.9706

Table C.9. Least squares equation coefficients of product yield (%) of STR No. 2, Series B experiments, with solid-liquid separation by 12-μm filters

	Raw data fit	[-1, +1] normalization	Sigma normalization
One-variable models			
R^2	0.561	0.078	0.561
Intercept	61.285	82.009	82.075
CT	2.883	-3.212	7.007
R^2	0.545	0.695	0.543
Intercept	308.562	89.807	82.075
TMP2	-0.178	-271.408	-6.893
Two-variable models			
R^2	0.762	0.787	0.762
Intercept	58.472	82.898	82.075
ET	-0.0006057	-5.439	-6.854
CTMP	3.289	31.909	4.585
R^2	0.759	0.759	0.759
Intercept	59.513	81.721	82.075
ET	-0.0006	-5.794	-6.557
COOH	112.009	5.6004	4.561
Three-variable models			
R^2	0.895	0.926	0.895
Intercept	52.938	82.887	85.075
ET	-0.0006506	-6.236	-7.363
CTMP	3.447	28.130	4.806
W2TMP	1.427	25.111	3.457
R^2	0.893	0.859	0.893
Intercept	54.375	77.713	82.075
W22	251.093	9.775	3.488
ET	-0.00067958	-7.244	-7.691
CTMP	3.480	35.464	4.851
Four-variable models			
R^2	0.976	0.776	0.976
Intercept	66.585	84.439	82.075
W2	-2168.742	0.145	-147.186
ET	-0.0008662	-6.101	-9.803
W2TMP	62.283	28.103	150.864
COOH2	299.424	-5.003	5.925
R^2	0.976	0.926	0.976
Intercept	48.387	82.890	82.075
W2	-1955.059	0.189	-132.684
ET	-0.0008690	-6.246	-9.835
CTMP	4.171	28.043	5.816
W2TMP	56.357	25.959	136.510

Table C.10. Least squares equation coefficients of product yield (%) of STR No. 2, Series B experiments, with solid-liquid separation by 1-μm filters

	Raw data fit	[-1, +1] normalization	Sigma normalization
	One-variable models		
R^2	0.508	0.029	0.508
Intercept	71.840	85.899	85.927
CT	1.953	-1.381	4.748
R^2	0.491	0.588	0.491
Intercept	239.232	90.989	85.927
TMP2	-0.120	-177.674	-4.666
	Two-variable models		
R^2	0.746	0.456	0.746
Intercept	84.820	85.180	85.927
ET	-0.0004328	-3.978	-4.858
CW2	214.3	-0.411	3.620
R^2	0.682	0.029	0.682
Intercept	68.783	85.894	85.927
CT	1.883	-1.389	4.576
CW2	165.088	-0.243	2.787

	Raw data fit	[-1, +1] normalization	Sigma normalization
	Three-variable models		
R^2	0.895	0.604	0.895
Intercept	86.697	85.062	85.929
ET	-0.0005948	-4.202	-6.732
CW2	501.965	-0.462	8.475
W2T	-2.582	-3.510	-5.617
R^2	0.888	0.892	0.888
Intercept	65.385	86.398	85.927
ET	-0.0004447	-4.363	-5.033
CTMP	2.295	16.670	3.200
W2TMP	1.340	22.963	3.245
	Four-variable models		
R^2	0.976	0.895	0.976
Intercept	61.984	86.385	85.927
W2	-1460.694	0.814	-99.137
ET	-0.0006091	-4.319	-6.880
CTMP	2.836	17.045	3.955
W2TMP	42.380	19.303	102.654
R^2	0.975	0.799	0.976
Intercept	74.382	87.700	85.927
W2	-1603.764	1.255	-108.843
ET	-0.0006057	-4.132	-6.856
W2TMP	46.346	19.405	112.263
COOH2	203.191	-3.637	4.021

The second type of equation that was chosen to fit the data redefined the variables so that the value of each variable in the equations varied from -1 to +1, while the value of each variable in the experiment changed from its minimum to maximum value. An example will clarify this defintion.

Consider the first three-variable [-1, +1] normalized equation for STR No. 1, Series B experiments, with solid-liquid separation by 12-μm filter, as shown in Table C.7. Here R^2 equals 0.884, intercept equals 72.652, $\overline{TMP}$ is 34.355, $\overline{WIT}$ is 4.869, and $\overline{TMP^2}$ is 3063.427. The equation is written as:

$$Y = 72.652 - (34.533 \times \overline{TMP}) + (4.969 \times \overline{WIT}) - (3063.427 \times \overline{TMP^2}) \quad . \quad (C.3)$$

Y is defined as the percent product yield. The other terms are defined in Table C.4 as:

$$\overline{TMP} = \frac{TMP - 37}{5} \quad , \quad (C.4)$$

$$\overline{WIT} = \left(\frac{W1 - 0.09}{0.09}\right) \times \left(\frac{T - 30}{10}\right) \quad , \quad (C.5)$$

$$\overline{TMP^2} = \left(\frac{TMP - 37}{5}\right)^2 \quad . \quad (C.6)$$

In the experiments, the temperature varies from 32 to 42°C (i.e., a range of 10°C), and time varies from 20 to 40 min (a range of 20 min). Similarly, stirrer speed varies from 0.02 to 0.20 W/liter with an operating range of 0.18 W/liter. If the values of any of these variables are put into Eqs. (C.4) to (C.6), the redefined variables vary from -1 to +1 over the experimental range. By examining Eq. (C.6), it can be clearly seen that of the variables investigated, TMP^2 (the temperature squared) is by far the most important. In contrast, the coupled effect of stirrer speed x reactor residence time is seen to be small. Fitting equations to this form allows the experimenter to weigh the relative importance of the various variables.

The equations were also written in a third form, which normalized the equations with the new variable form shown below:

$$\bar{\bar{X}} = \frac{X - X \text{ mean}}{\sigma} \quad , \quad (C.7)$$

where

$\bar{\bar{X}}$ = variable to use in equations with coefficients listed in Tables C.6, C.7, C.9, and C.10;

X = experimental value of variable;

X_{mean} = average value of variable X in a series of experimental runs,

σ = standard deviation of X.

This type of normalization, although not as easy to comprehend, does offer some significant advantages:

1. The normalization technique guarantees that each variable is on an equal basis. If particular variables were not held to their exactly desired value in some experiments, this type of analysis automatically compensates by changing sigma.
2. If some variable that was to be held constant actually varies, this normalization method allows that variable to be analyzed as an additional variable to determine if the unexpected changes are important.

C.2 Least Squares Fit of STR No. 1, Series B Experiments

Examination of Tables C.4, C.6, and C.7 reveals several important relationships between the variables and product yield from STR No. 1 in Series B experiments. The most important observations are the following:

1. Temperature is an important, nonlinear variable of product yield. In Table C.3, temperature is the most important one-variable parameter. This is particularly significant because unlike Series A experiments, Series B experiments had "constant temperature." In effect, temperature controller noise became the dominant variable. Because $[TMP]^2$ is more significant than [TMP] and because the coefficient of $[TMP]^2$ is negative, increasing temperature rapidly decreases product yield. Near the operating temperature of 35°C, a rise in temperature can cause a major reduction in product yield.

2. Time as a variable of product yield is best represented in the variable form $1 - e^{-t}$ or $1 - e^{-AT}$. Time was allowed to enter the equations in three forms — T, T^2, and e^{-t}. The form e^{-t} produced the best correlations, as shown in Table C.3.

3. As evident earlier, stirrer power for STR No. 1 is not a major variable. Stirrer power enters into the equations, but the coefficients are generally small.

C.3 Least Squares Fit of Product Yield of Series B Experiments

Tables C.8, C.9, and C.10 give the results of the least squares analysis of product yield for the final product from Series B experiments. Two important results are evident:

1. Temperature is an important, nonlinear, negatively correlated variable of product yield. The results are similar to those discussed in Sect. C.2. Table C.2 shows the raw data and the relatively small temperature effects that were found significant.

2. Time as a variable of product yield is best represented in the variable form $1 - e^{-t}$ or t^2.

THIS PAGE

WAS INTENTIONALLY

LEFT BLANK

Appendix D. HOMOGENEOUS PRECIPITATION WITH SIMULTANEOUS CRYSTAL SEPARATION

THIS PAGE

WAS INTENTIONALLY

LEFT BLANK

Appendix D. HOMOGENEOUS PRECIPITATION WITH SIMULTANEOUS CRYSTAL SEPARATION

A very short series of exploratory experiments were conducted using diethyl oxalate as the source of oxalic acid for precipitation of lanthanides. The equipment flowsheet is shown in Fig. D.1, and the main reaction vessel is shown in Fig. D.2. In this process, the synthetic waste feed solution was mixed with water and diethyl oxalate and sent to the crystallizer. The crystallizer consisted of a straight glass tube down the center of a tapered column. The liquid entered the center straight tube, traveled down the tube and then up the tapered column to the exit. Ideally, crystals are formed in the tapered column and drop to the bottom of the column. The column is heated at the top and cooled at the bottom. This high temperature gradient provides stability against unwanted mixing in the crystallizer.

The diethyl oxalate in the presence of water hydrolyzes to oxalic acid and ethanol. The result is a slow increase with time in oxalic acid concentration in the presence of the waste feed solution. The rate of hydrolysis is dependent upon temperature and acid concentration. Some previous experiments (ref. 24, Sect. 6) have suggested that slowly increasing oxalic acid concentrations with time should improve product yields of actinides through a process called carrier precipitation.

Examination of the product yield in Table D.1 shows very low product yields for the exit streams (7.7 to 15.8%) but shows moderate yields when the exit streams are filtered with 1-μm filters (41.1 to 73.9%). The crystals collected from the bottom of the crystallizer were about five times the size of crystals from the STRs but were few in number.

The product yields for various sizes of filters vary greatly but exhibit little pattern with respect to the two main operating variables — time and temperature. At low operating temperature, increased reactor residence time improved product yields, whereas the reverse was true at higher temperatures. The considered explanation of these results is as follows. Diethyl oxalate requires time to dissociate; hence, with greater times, more oxalic acid is formed with higher product yields. Diethyl

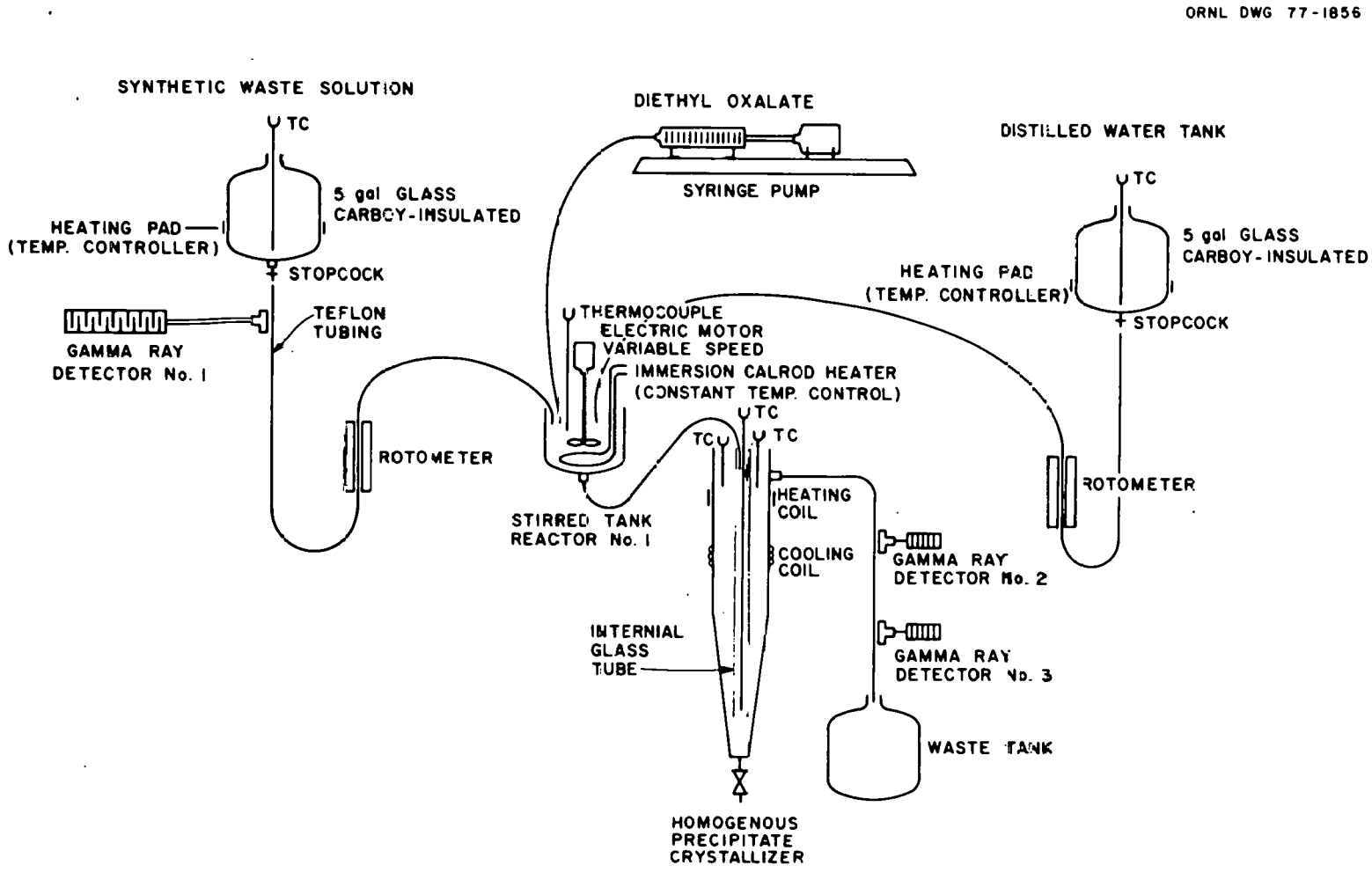

Fig. D.1. Experimental equipment arrangement for homogeneous precipitation using diethyl oxalate.

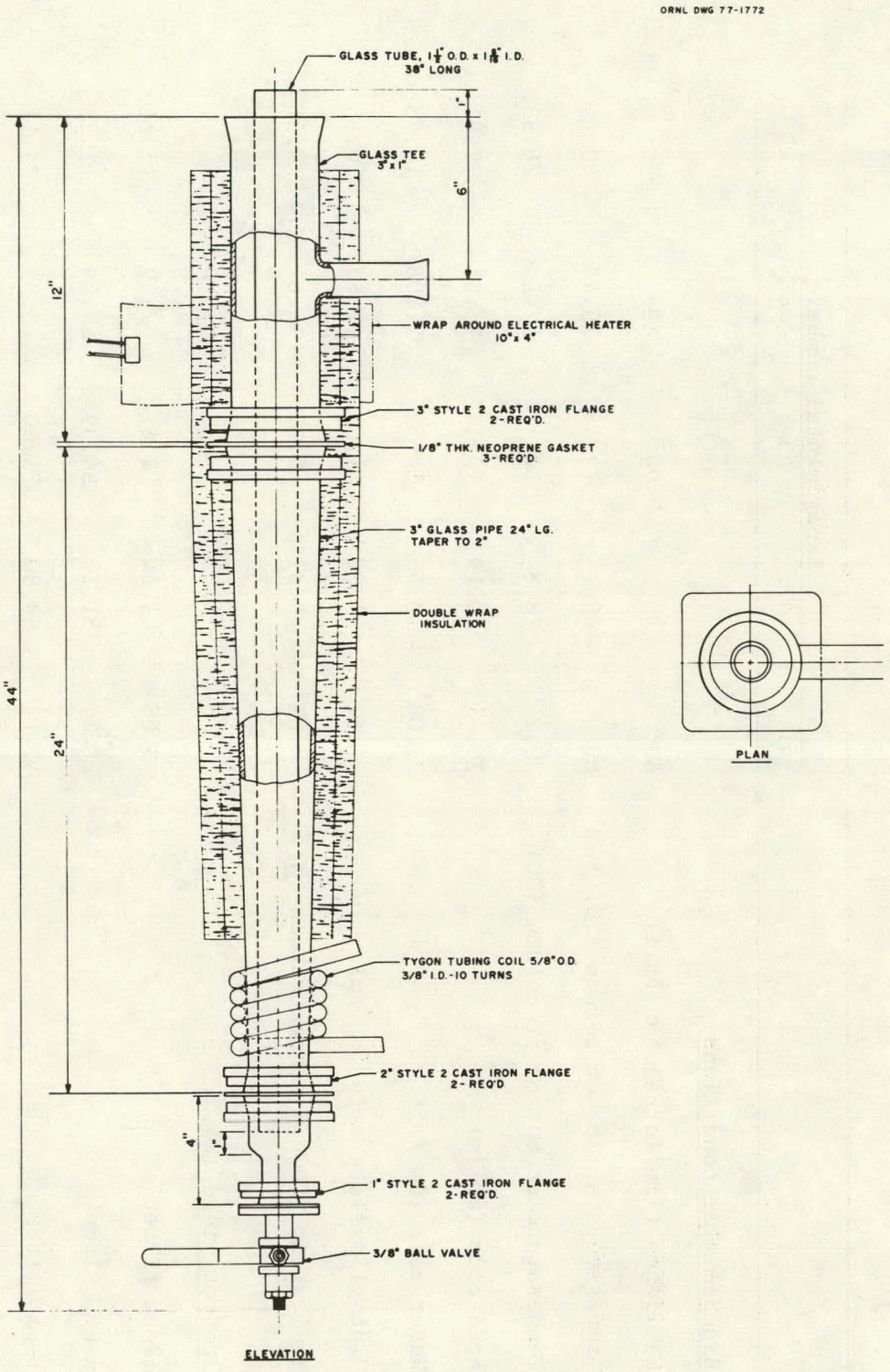

Fig. D.2. Homogeneous precipitator crystallizer.

Table D.1. Initial experimental conditions and product yields obtained in the homogeneous precipitate experiments

	Experimental number				
	41	42	43	44	45
Experimental conditions					
Residence time in reactor (min)	60	90	90	60	120
Temperature at top of column (°C)	60	60	79.45	79.45	60
Temperature at bottom of column (°C)	30.2	28.8	30	32.6	26.9
Feed rate (cm^3/m)	15.31	10.19	10.19	15.31	7.81
Water rate (cm^3/m)	27.08	18.55	18.55	27.08	14.58
Diethyl oxalate rate (cm^3/m)	1.67	1.08	1.08	1.67	0.85
Equivalent $(COOH)_2$ concentration (M)	0.31	0.31	0.31	0.31	0.31
Product yield (%)					
12-μm filter	5.68	11.24	2.31	7.49	-15.11
5-μm filter	21.84	51.17	34.39	60.24	71.27
1-μm filter	41.11	69.60	71.50	73.93	75.11
Exit stream	15.13	12.31	7.71	15.84	10.22

oxalate is, however, a fairly volatile compound. At higher temperatures it is probably being distilled out of the water before it dissociates into oxalic acid.

The above results are of a preliminary nature. Considering the poor results, however, the concept (diethyl oxalate in a downflow-upflow crystallizer) is probably not worth further effort unless much longer reactor residence times for the wastes are acceptable. Long reactor residence times can, unfortunately, result in significant oxalate decomposition from radiation; hence, there are technical questions on the feasibility of this approach. Although the apparatus may be worth additional investigation as a settler, there are serious questions about the feasibility of settlers for this solid-liquid separation task.

THIS PAGE

WAS INTENTIONALLY

LEFT BLANK

ORNL/TM-6445
Dist. Category UC-70

INTERNAL DISTRIBUTION

1. C. W. Alexander
2. J. O. Blomeke
3. W. D. Bond
4. W. D. Burch
5. D. O. Campbell
6. B. C. Finney
7-16. C. W. Forsberg
17. H. R. Gwinn
18. A. L. Harkey
19. F. A. Kappelmann
20. R. E. Leuze
21. K. H. Lin
22. A. L. Lotts
23. F. M. Scheitlin
24. R. R. Shoun
25. L. M. Toth
26. B. L. Vondra
27. R. G. Wymer
28-29. Central Research Library
30-34. Laboratory Records
35. Laboratory Records, R.C.
36. ORNL—Y-12 Technical Library Document Reference Section
37. ORNL Patent Section
38. G. R. Choppin (consultant)

EXTERNAL DISTRIBUTION

39-40. Director, Division of Nuclear Power Development, Department of Energy, Washington, DC 20545
41. Office of Assistant Manager, Energy Research and Development, Department of Energy, Oak Ridge Operations Office, Oak Ridge, TN 37830
42. Director, Nuclear Research and Development Division, Department of Energy, Oak Ridge Operations, Oak Ridge, TN 37830
43. H. Babad, Atlantic Richfield Hanford Company, P.O. Box 250, Richland, WA 99352
44. Ralph Best, Battelle Columbus Laboratories, 505 King Ave., Columbus, OH 43201
45. J. A. Buckham, Allied-General Nuclear Services, P.O. Box 847, Barnwell, SC 29812
46. J. L. Burnett, Department of Energy, Washington, DC 20545
47. R. E. Burns, George C. Marshall Space Flight Center, Marshall Space Flight Center, AL 35812
48. N. E. Carter, General Manager, Battelle Memorial Institute, Office of Nuclear Waste Isolation, 505 King Ave., Columbus, OH 43201
49. R. Cooperstein, U.S. Nuclear Regulatory Commission, Washington, DC 20555
50. J. L. Crandall, Director of Planning, Savannah River Laboratory, Aiken, SC 29801
51. R. Danford, Input Processing Division, Institute Research and Evaluation, 21098 IRE Control Center, Eagen, MN 55121
52. J. P. Duckworth, Nuclear Fuel Services, Inc., P.O. Box 124, West Valley, NY 14171

53. E. S. Goldberg, Chief of Waste Management, Savannah River Operations Office, P.O. Box A, Aiken, SC 29801
54. L. R. Hill, Sandia Laboratories, P.O. Box 5800, Albuquerque, NM 87115
55. E. P. Horwitz, Argonne National Laboratory, 9700 South Cass Ave., Argonne, IL 62439
56. D. E. Large, Department of Energy, Oak Ridge Operations, Oak Ridge, TN 37830
57. H. Lawroski, Allied Chemical Corp., P.O. Box 2204, Idaho Falls, ID 83401
58. R. E. Lerch, Hanford Engineering Development Laboratory, P.O. Box 1970, Richland, WA 99352
59. W. J. Maraman, Los Alamos Scientific Laboratory, P.O. Box 1663, Los Alamos, NM 37544
60. J. Martin, Director for Waste Management, Division of Fuel Cycle and Material Safety, U.S. Nuclear Regulatory Commission, Washington, DC 20555
61. G. W. Mason, Argonne National Laboratory, 9700 South Cass Ave., Argonne, IL 62439
62. G. J. McCarthy, Pennsylvania State University, Materials Research Laboratory, University Park, PA 16802
63. L. D. McIsaac, Allied Chemical Corp., P.O. Box 2204, Idaho Falls, ID 83401

64-66. G. Oertel, Director, Division of Waste Products, Office of Nuclear Waste Management, Department of Energy, Washington, DC 20545

67. D. A. Orth, Savannah River Plant, E. I. du Pont de Nemours & Co., Inc., Aiken, SC 29801
68. A. M. Platt, Pacific Northwest Laboratory, P.O. Box 999, Richland, WA 99352
69. M. Pobereskin, Battelle Columbus Laboratories, 505 King Ave., Columbus, OH 43201
70. W. W. Schulz, Atlantic Richfield Hanford Company, P.O. Box 250, Richland, WA 99352
71. J. J. Shefcik, General Atomic Company, P.O. Box 81608, San Diego, CA 92138
72. M. J. Steindler, Argonne National Laboratory, 9700 South Cass Ave., Argonne, IL 60439
73. G. H. Thompson, Rockwell International, Rocky Flats Plant, P.O. Box 464, Golden, CO 80401
74. R. E. Tomlinson, Manager, Exxon Nuclear Company, Inc., 2101 Horn Rapids Rd., Richland, WA 99352
75. R. D. Walton, Department of Energy, Washington, DC 20545
76. E. J. Wheelwright, Battelle Northwest Laboratory, P.O. Box 999, Richland, WA 99352
77. A. Bathelier, Commissariat a l'energie Atomique, B.P. No. 6, Fontenay-aux-Roses, France
78. J. Grover, AERE, Harwell, Didcot, Oxfordshire OX 11 ORQ, England
79. F. Girardi, CCR Euratom, I-21020, Ispra, Italy
80. H. Haug, Kernforschungszentrum Karlsruhe, Postfach 3640, D-75 Karlsruhe, Germany

81. G. N. Kelly, National Radiological Protection Board, Harwell Didcot, Oxfordshire OX 11 ORQ, England
82. J. O. Liljenzin, Chalmers University of Technology, Fack, S-402 20, Göteborg, Sweden
83. K. J. Schneider, IAEA, P.O. Box 590, A-1011 Vienna
84. L. Tondinelli, Comitato Nazionale per l'Energia Nucleare, Lab. Teoria e Calcolo Reattori, 00100 Roma, Italy
85. D. W. Tedder, Georgia Institute of Technology, School of Chemical Engineering, Atlanta, GA 30332

86-409. Given distribution as shown in TID-4500 under Nuclear Waste Management category

☆U.S. GOVERNMENT PRINTING OFFICE: 1979-640-079/354